Graduate School of Biological Sciences　Doctoral Thesis Abstract

| Lab name (Supervisor) | Laboratory of Molecular Immunobiology (Professor Taro Kawai) | | |
|---|---|---|---|
| Name (surname) (given name) | Zainol, Mohd Izwan | Date | 19/09/13 |
| Title | Innate immune responses through Toll-like receptor 3 (TLR3) require RNA-binding protein HuR-mediated Atp6v0d2 mRNA stabilization | | |


Abstract

The innate immune system comprises various pattern-recognition receptors (PRRs), which recognize conserved microbial components known as pathogen-associated molecular patterns (PAMPs) to protect the host from pathogen invasion. Among PRRs, Toll-like receptors (TLRs) is one of the well-characterized PRRs consisting of more than ten functional members in mammals, each with a specific PAMP recognition ability. TLR3 recognizes double-stranded RNA derived from virus and its synthetic analogue, polyinosinic-polycytidylic acid, poly(I:C). TLR3 is primarily localized in endosomes, and the endosomal localization is essential for its activation via the proteolysis and dimerization, which is controlled by mechanisms involving endosomal pH. Upon poly(I:C) binding, TLR3 exclusively recruits an adaptor protein, TRIF (TIR-domain-containing adapter-inducing interferon-β, also known as TICAM1) and eventually activates transcription factors NF- κB and IRF3, to conduct the production of inflammatory cytokines and type I interferon, respectively.

Human Antigen R (HuR) is one of the RNA binding proteins (RBPs) which recognizes the 3′ untranslated region (3′UTR) of target mRNAs, thereby protecting them from immediate mRNA degradation. Specifically, it recognizes Adenylate-uridylate-Rich Elements (AREs) which consist of multiple copies of the specific pentamer sequence "AUUUA". Through conserved RNA Recognition Motifs (RRMs), HuR forms a protein-mRNA complex which shuttles between nucleus and cytoplasm, providing target mRNA with ongoing protection from the degradation machinery. To date, there are limited data on post-transcriptional regulation of gene expression during innate immune responses.

Here, I found that HuR-deficient murine macrophage cells showed a significant reduction

in *Ifnb1* and *Cxcl10* mRNAs expression after poly(I:C) stimulation. Stimulation of cells with R837 and ODN1668, synthetic ligands for TLR7 and TLR9 respectively, however, showed no defective responses with regards to *Ifnb1* and *Cxcl10* mRNAs expression. Consistent with data on HuR KO cells, HuR knocked down MEF cells, and RAW264.7 cells also exhibited a significant reduction of *Ifnb1* and *Cxcl10* mRNA after stimulation with poly(I:C) as compared with scramble shRNA treated cells. The phosphorylation of IRF3 was lower after poly(I:C) stimulation in HuR KO cells than in WT cells.

It noted that RT-qPCR analysis indicated a significant reduction of the expression of *Atp6v0d2*, a subunit of vacuolar-type $H^+$ ATPase (V-ATPase) in HuR KO cells. Acridine orange staining of HuR KO cells demonstrated a reduction in endosomal acidification as compared to WT cells. The *Ifnb1* and *Cxcl10* mRNA levels were increased after poly(I:C) stimulation when FLAG-Atp6v0d2 was expressed in HuR KO cells when compared with HuR KO cells. Using RNA immunoprecipitation (RIP) assay, I found that HuR associated with 3′UTR in *Atp6v0d2* mRNA. HuR interacted with AREs of *Atp6v0d2* mRNA at nucleotides 1867–1921 and 2101–2155 within 3′UTR. Actinomycin D treatment demonstrated that the stability of *Atp6v0d2* mRNA was sustained by HuR association.

Taken these results together, HuR plays a critical role in facilitating TLR3-mediated innate immune response via post-transcriptionally regulation of the stability of mRNAs crucial in endosomal pH maintenance such as *Atp6v0d2* mRNA.

Doctoral Thesis

# Innate immune responses through Toll-like receptor 3 (TLR3) require RNA-binding protein HuR-mediated *Atp6v0d2* mRNA stabilization

Mohd Izwan Bin Zainol

Nara Institute of Science and Technology

Graduate School of Biological Sciences (Laboratory of Molecular Immunobiology)

(Professor Taro Kawai)

2019 September 13th

## Table of Contents

# 1. Introduction

## 1.1. Innate immunity: Toll-like receptors (TLRs) family

The vital role of the innate immune system is to detect the presence of infectious pathogens and subsequently initiates the elimination mechanism to protect the host from pathogen invasion. The pathogen sensing by the host is achieved via germline-encoded pattern-recognition receptors (PRRs), which recognize conserved microbial components known as pathogen-associated molecular patterns (PAMPs) in both extracellular and intracellular regions. Toll-like receptors (TLRs) are firstly investigated PRRs family, which consists of more than ten members in mouse and human (Fig. 1). Each member detects specific PAMPs such as lipoproteins (LTA) (TLR1, TLR2, and TLR6), double-stranded RNA (dsRNA) (TLR3), lipopolysaccharides (LPS) (TLR4), flagellin (TLR5), single-stranded RNA (ssRNA) (TLR7, TLR8, and TLR13) and double-stranded DNA (TLR9) (C. C. Lee, Avalos, and Ploegh 2012). In general, TLRs contain leucine-rich repeats responsible for recognizing their cognate PAMPs at their ectodomains. Their transmembrane domain, which contains intracellular Toll-interleukin 1 (IL-1) receptor (TIR) domain is crucial in downstream signal transduction. TLRs usually recognize their respective PAMPs in a membrane-bound cellular compartment such as plasma membrane, endosome, and lysosome as a type I transmembrane proteins. Most TLRs activate Myeloid differentiation primary response 88 (MYD88) as their downstream adaptor molecule, except only for TLR3 which recruits TIR-domain-containing adapter-inducing interferon-β (TRIF, also known as TICAM-1) as it's downstream adaptor. Regardless, both pathways lead to the activation of transcriptional factor; Nuclear Factor kappa-B (NF-κB) and various Interferon Regulatory Factors (IRFs) by nuclear translocation, which eventually induces the production of type I interferon and inflammatory cytokines (Kawai and Akira 2010).

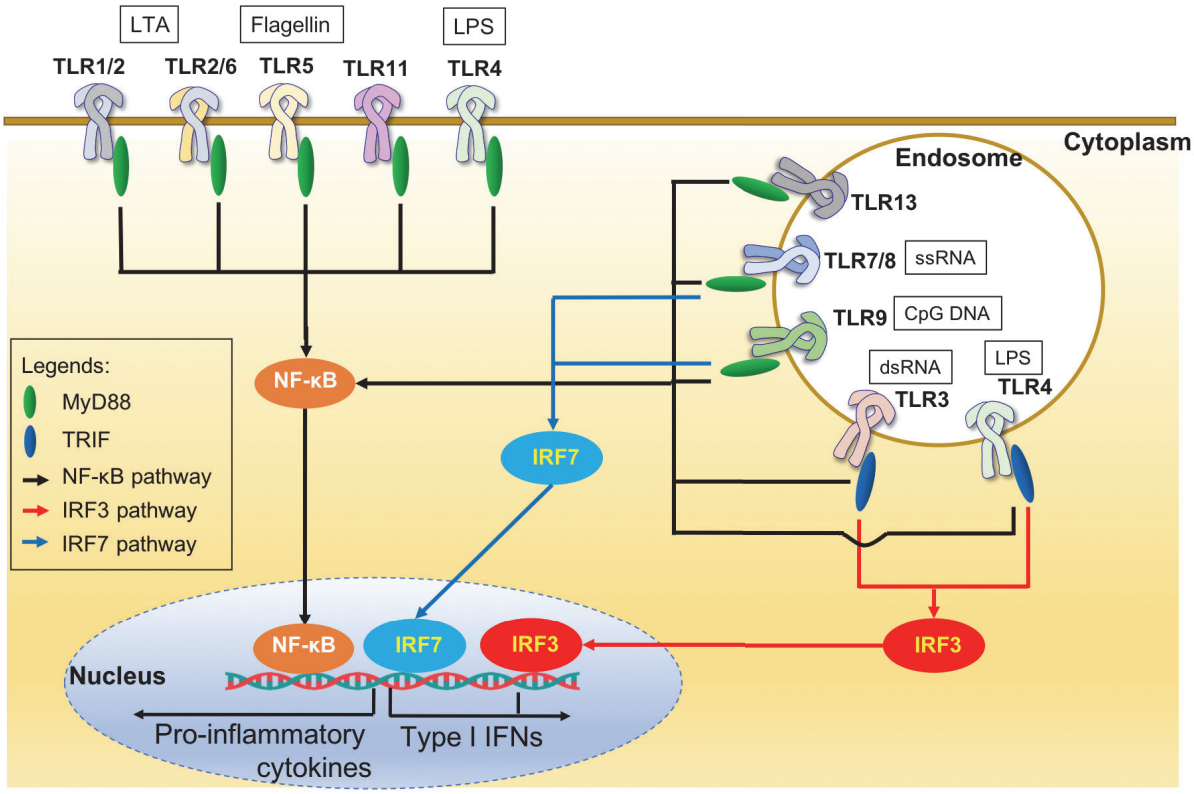


**Figure 1.** Toll-like receptors (TLRs) family is generally subdivided into two major subgroups based on their cellular localization and respective PAMPs. The cell surface TLRs which recognize microbial membrane structure include TLR1, TLR2, TLR4, TLR5, TLR6, and TLR11. The other group consists of TLR3, TLR7, TLR8, TLR9 and TLR13 localizing in intracellular vesicles like endosomes and mainly recognizes microbial nucleic acids. Most TLRs recruit MyD88 as their downstream adaptor protein upon activation except for TLR3 and internalize TLR4 which recruit TRIF as their alternative downstream adaptor molecule.

## 1.2. Endosomal TLRs: TLR3

TLR3, TLR7, TLR8, TLR9 and TLR13, which recognize nucleic acids, are primarily localized in endosomes (Gleeson 2014). Endosomal localization functions to prevent from autoimmune or inflammatory disorders by discriminating between self-DNA or -RNA (Diebold and Brencicova 2013). Infectious pathogens like viruses and bacteria typically enter cells through endocytic or phagocytic pathways and reached to the endosome where they are recognized by TLRs members. The endosomal localization of TLRs is essential for their activation via the proteolysis and dimerization, which is controlled by several mechanisms such as endosomal pH and transportation by UNC93B1. TLR3, TLR7, and TLR9 are primarily synthesized in the endoplasmic reticulum (ER) and transported to endosome with

the aids of UNC93B1 chaperone protein. It is required by endosomal TLRs for trafficking (Fig. 2). Defective UNC93B1 was reported to prevent endosomal TLRs from leaving ER (Brinkmann et al. 2007; Kim et al. 2008). Its expression is required for endosomal TLR activation and signaling (Garcia-Cattaneo et al. 2012). Proteolytic cleavage by cathepsins or asparagine endopeptidase (AEP) in the endosome is crucial for ligand binding efficiency and is thought to prevent endosomal TLRs contact with self-nucleic acids in extracellular fluid, otherwise causing autoimmunity (B. L. Lee and Barton 2014).

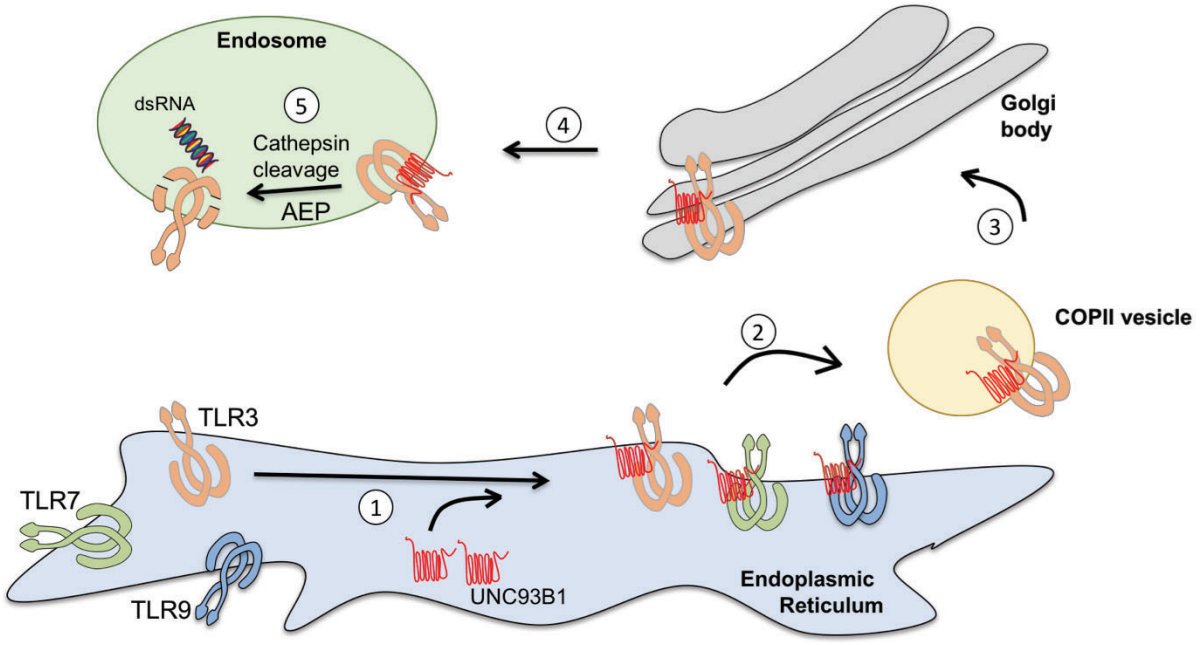


**Figure 2.** Endosomal TLRs transportation by UNC93B1 from ER to endosome. (1) The assembly of UNC93B1 and TLRs occurs in ER. (2) UNC93B1-bound TLR is transported via COPII vesicle into Golgi body (3). Finally, the TLR-UNC93B1 complex reaches to the endosome and under acidic condition, permits the cleavage of TLRs by cathepsin and AEP into a mature form that can bind to the ligand (5).

TLR3 specifically recognizes dsRNA derived from viruses as well as Polyinosinic: polycytidylic acid [(Poly I:C)], a synthetic RNA analogue mimicking dsRNA (H. Kumar, Kawai, and Akira 2009). Ligands recognition by TLR3 occurs in a sequence-independent manner of viral genomic dsRNA. Minimum length of dsRNA for TLR3 recognition is 45

base pairs (bp) with higher pro-inflammatory induction by >90 bp dsRNA. This feature of TLR3-ligand binding capacity enables to discriminate between infectious viral dsRNA and small interfering RNA (siRNA) molecules. The ability of TLR3 to distinguish between pathogen and self-nucleic acids is more prominent as compared to other endosomal TLRs due to limited self-dsRNA in mammalian cells (Vercammen, Staal, and Beyaert 2008). There are only a few short structures of self-dsRNA available among eukaryotic cells RNA such as the secondary clover-leaf structure of transfer RNA (tRNA) or micro RNA (miRNA) as well as small hairpin RNA (shRNA) (Diebold and Brencicova 2013). TLR3, as mentioned earlier, recruits TRIF as its downstream adaptor protein, which subsequently activates downstream signaling pathway via phosphorylation and nuclear translocation of transcription factors NF-κB and IRF3. These activations result in the production of pro-inflammatory cytokines and type I interferons respectively, which are the key mediators for innate antiviral immunity.

### 1.3. Poly(I:C) stimulation: TLR3 and RLR signaling pathways

Viral infection activates two distinct pathways of the host innate immune system; namely, membrane-bound TLR pathway via endosomal TLR3 and cytoplasmic RIG-I-like Receptor (RLR) pathway. RLR pathway includes RNA helicase retinoic acid-inducible gene – I (RIG-I) receptor and melanoma differentiation-associated gene 5 (MDA5). Both pathways possess similar characteristics such as response to dsRNA ligand, propagate homotypic interaction and resulting in NF-κB and IRF3 activations, which subsequently initiate the production of pro-inflammatory cytokines and type-I interferons (IFNs) (Fig. 3). Homotypic interaction of TLR3 involves TIR domain that conserved in both TLR3 and its downstream TRIF adaptor molecule. RLR homotypic interaction utilizes caspase recruitment domain (CARD) possesses by RIG-I/MDA5 and their interacting partner, mitochondrial IPS-1 molecule (Meylan and Tschopp 2006). Specifically, TLR3 recognizes dsRNA ligand ranging between 39 and 139 bp in length dependable to their site of encounters in early or late

endosome (Leonard et al. 2008). RIG-I generally detects short cytosolic dsRNA and 5′-triphosphate single strand (ss)-RNA, whereas MDA5 recognizes long cytosolic dsRNA (Barral et al. 2009; Jensen and Thomsen 2012). The route of ligand delivery is suggested to be the determining factor to activate those antivirals PRRs. Study using poly(I:C) stimulation delivered in the form of liposome-encapsulated ligand has been shown that transfected poly(I:C) is more effective in activating RLR pathway in numerous cell types such as fibroblast and epithelial cells (Dauletbaev et al. 2015).

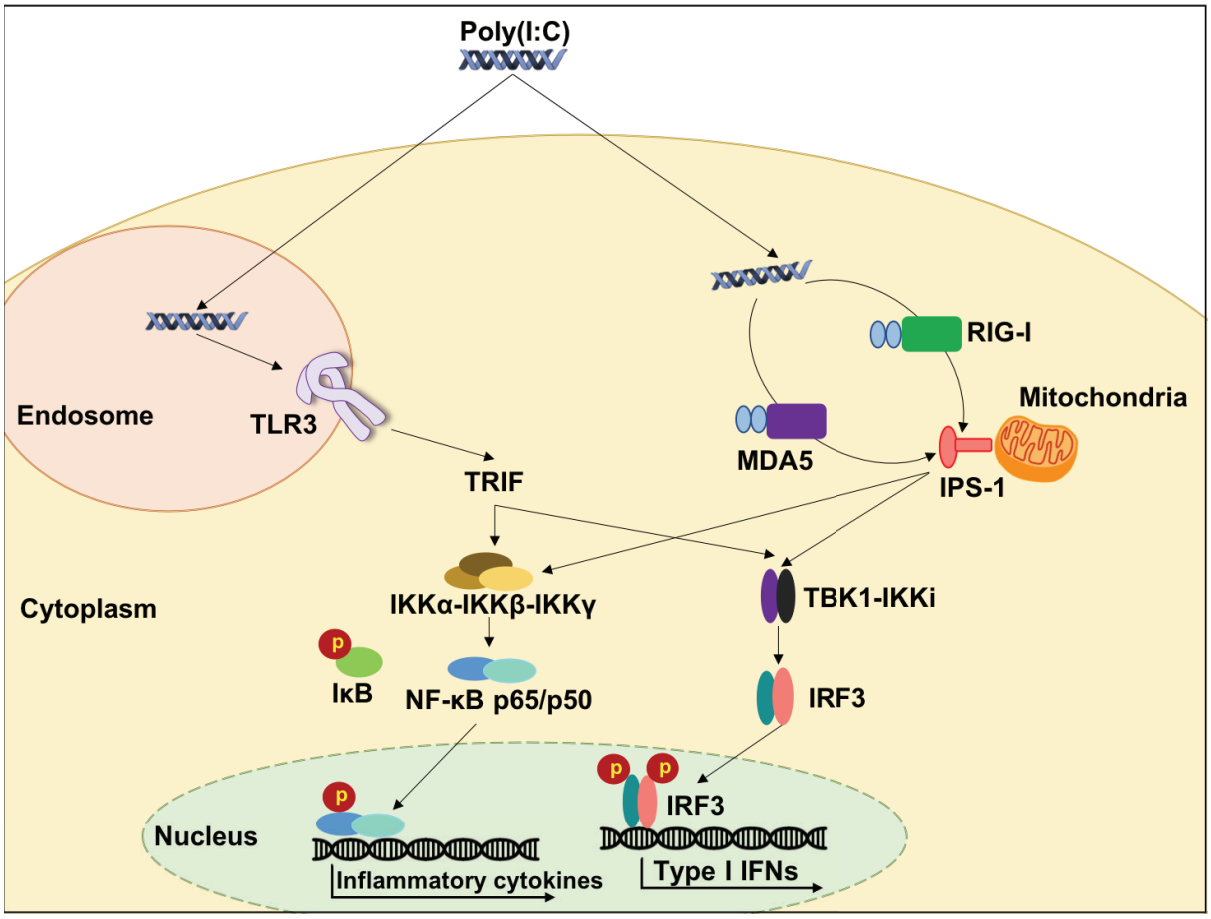


**Figure 3.** TLR3 and RLR pathways following poly(I:C) stimulation. On the left side, TLR3 recognizes poly(I:C) in endosome and become activated to recruit TRIF. Activated TRIF molecule interacts with its downstream targets, namely IKKs complex to relay signals to phosphorylate NF-κB and translocate it into the cytoplasm to induce transcription of inflammatory cytokines. TRIF also acts on TBK1-IKKi complex to activate and phosphorylate IRF3, which then translocated into the nucleus for the production of type 1 IFNs. RLR pathway involves poly(I:C) cytosolic detection by RIG-I or MDA5 which activates mitochondrial IPS-1, then subsequently activate both arms of IKKs complex and TBK1 to phosphorylate NF-κB and IRF3 and translocate them into the cytoplasm.

## 1.4. RNA-Binding Proteins: HuR

Eukaryotic cells initiate their protein expression from genetic materials by synthesizing mRNA in the nucleus. A critical feature of mRNA which determines their cytosolic fate is their instability at physiological conditions which can be manipulated through the formation of ribonucleoprotein (RNP) complex. In order to form RNP complex, RNA-binding proteins (RBPs) specifically recognize RNA recognition motifs (RRM) by RNA binding domains such as hnRNP K homology domain (KH), zinc fingers, and DEAD-box helicase domain. In *Saccharomyces cerevisiae*, 70% of synthesized mRNA has been associated with at least one out of 40 identified RBPs (Hogan et al. 2008). Meanwhile, individual RBP was demonstrated to share multiple mRNA targets. It was also demonstrated that single mRNA could be targeted for numbers of different RBPs at a particular time. The interaction between RBP and target mRNA in cell culture is robustly dynamic.

Human Antigen R (HuR) also known as ELAV (embryonic lethal, abnormal vision, Drosophila)-like protein 1 (Elav-l1) is one of the ubiquitously expressed RBPs. In mammals, there are four highly conserved members of this family, namely, HuR (HuA/Elav-l1), HuB (Elav-l2), HuC (Elav-l3,) and HuD (Elav-l4). Predominantly, HuR mainly resides in the nucleus but can shuttle between the nucleus and cytoplasm through its nucleocytoplasmic domains upon various stress conditions. It is suggested that phosphorylation and methylation of HuR may play roles in initiating HuR-mRNA interaction, hence promoting their translocations (Katsanou et al. 2009). HuR primarily recognizes and binds to AU-rich elements (AREs) of target mRNA. Most AREs consist of multiple copies of the specific pentamer sequence "AUUUA". Their primary location is in the 3′UTR region of target mRNA. HuR, like other Hu proteins, is composed of 3 highly conserved RNA Recognition Motifs (RRMs) (Fig. 4). N-terminal RRM1 and RRM2 are essential in recognizing and binding mechanism of ARE of target mRNA. Hinge region, separating RRM1 and two from RRM3 at the C-terminal contains HuR nucleoplasmic shuttling (HNS) sequence crucial for HuR movement between nucleus and cytoplasm (Hinman and Lou 2008). Although earlier

studies suggested a negligible functionality, it was reported that RRM3 was required to assist oligomerization of HuR and promote RNA interaction by binding to Poly(A) tail of target mRNA (Scheiba et al. 2014).

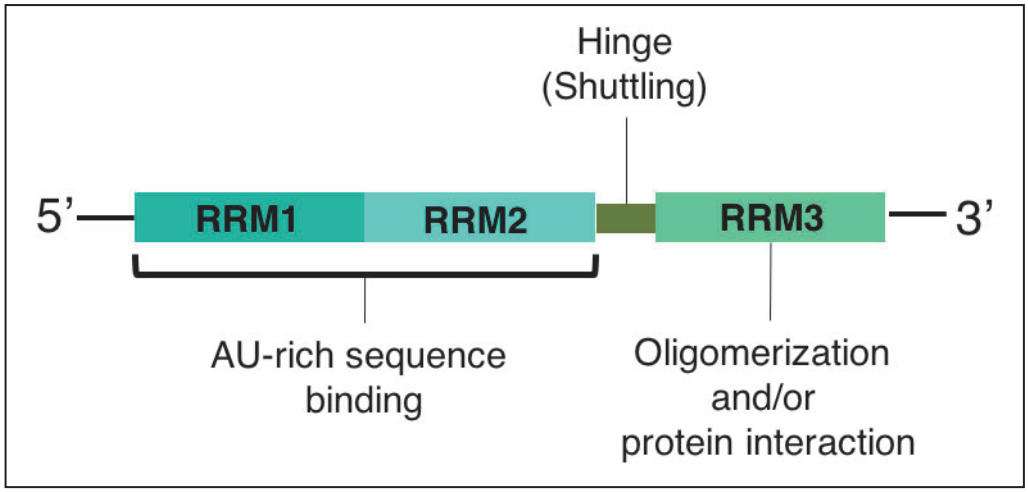


**Figure 4.** Domain architecture of HuR. Hu protein, in general consists of three RNA Recognition Motifs (RRMs). RRM1 and RRM2 are positioned adjacent to each other at N-terminal, which function to recognize and bind AU-rich sequence of target mRNA. RRM3 is located at C-terminal, separated from other RRM domains by hinge gap and important in oligomerization as well as protein interaction. Hinge gap is suggested to play a role in nuclear-cytoplasmic shuttling activity.

### 1.5. ATPase and innate immune response: Atp6v0d2

The vacuolar-type $H^+$ adenosine triphosphatase (V-ATPase) plays a pivotal role in the control of pH in intracellular compartments. Their function as proton pumps is required to maintain acidic conditions of endocytic components which are crucial for cellular activities such as enzymatic cleavage, receptor activation, ligand recognition and protein degradation (Maxson and Grinstein 2014). They are ubiquitously localized in a variety of intracellular structures including endosomes, lysosomes, Golgi-derived vesicles, synaptic vesicles, clathrin-coated vesicles, and chromaffin granules. V-ATPase is a multimeric complex structure consist of cytoplasmic $V_1$ sector as ATP hydrolysis components and transmembrane $V_0$ sector for their proton translocation machinery. $V_1$ sector contains eight different subunits

($A_3$, $B_3$, C, D, E, F, $G_2$, and $H_{1-2}$) while $V_0$ consists of six subunits (a, $c_4$, c', c", d, and e) (Marshansky and Futai 2008). It transports proton against electrochemical gradient across the membrane via a rotary mechanism which utilizes conserved glutamic acid as their proton transporter (Cotter et al. 2015). The energy required for the 360º rotation is provided by ATP hydrolysis by $V_1$ domain (Cross and Muller 2004). ATP hydrolysis causes a conformational change of A/B subunit, leading to the rotation of the central stalk, which in turn, rotates the membrane-embedded $V_0$ domain to allow $H^+$ to pass through the membrane via glutamic acid protonation (Fig. 5). The function of the $V_0$ domain remains unclear, but specific inhibitors such as bafilomycin, concanamycin, and lobatamides were reported to inhibit the rotation of $V_0$ domain (Huss and Wieczorek 2009).

$V_0$ domain of V-ATPase comprises of six subunits, with stoichiometry in yeast subunits a, c, c′, c″, d, and e (Fig. 5). Cytosolic proton is transported through rotating subunits c, c′ and c″ located at proteolipid ring, to protonate glutamic acid. The existing proton is then transferred to arginine residue in subunit a, and eventually released into endocytic lumen (Huss and Wieczorek 2009). Currently, limited data are available describing the function and contribution of subunit d and e of V-ATPase in cellular activity. Our previous study reported that subunit d of $V_0$ (Atp6v0d2) was required for innate immune response by endosomal TLRs (TLR3, 7 and 9) (Murase et al. 2018). Atp6v0d2 deficiency resulted in endosomal neutralization, hence abrogated cytokines production by these TLRs. Acidic condition is important for endosomal TLRs activation (Blasius and Beutler 2010; Chaturvedi and Pierce 2009; B. L. Lee and Barton 2014). It is generally accepted that V-ATPase plays an essential part in establishing acidic pH of intracellular compartments (Forgac 2007; Marshansky and Futai 2008; Mellman and Warren 2000; Murase et al. 2018; Sun-Wada, Wada, and Futai 2004). However, the process that underlines the pH control mechanisms remains elusive.

Atp6v0d2 may play important roles in acidification of endocytic structures as possessed by other $V_0$ subunit, thus warrant further investigations.

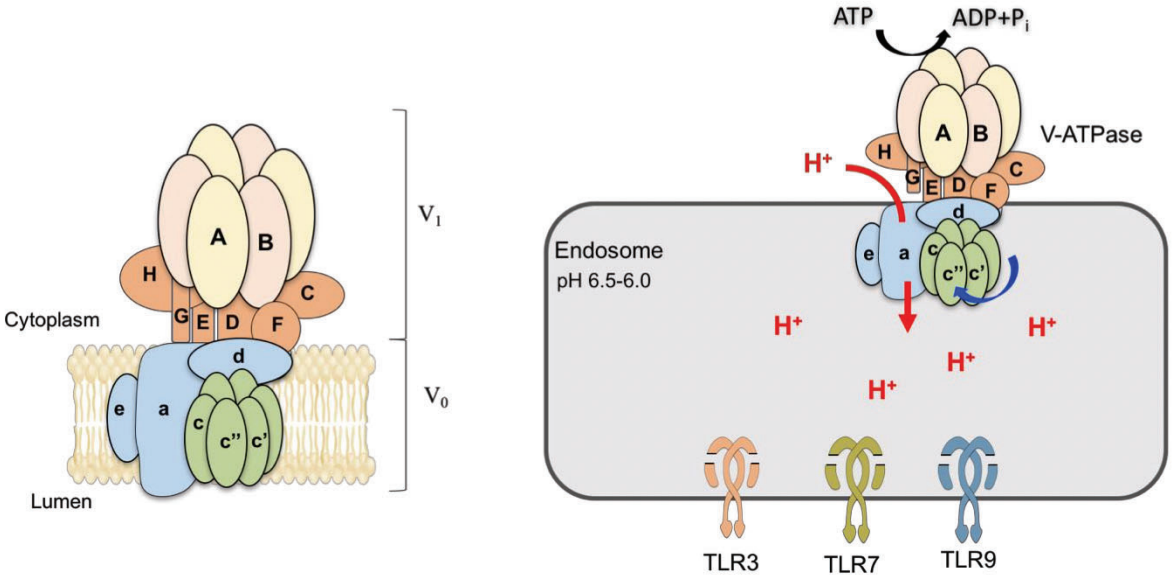


**Figure 5.** Structure of V-ATPase (adapted from Forgac, 2007) (left). V1 is a peripheral domain responsible for ATP hydrolysis while Integral transmembrane $V_0$ domain is involved in proton translocation across the membrane into the lumen of endosome. The right panel shows ATP-dependent mechanism of V-ATPase as a proton pump to maintain the acidic condition of endosome and facilitates TLRs activation.

## 1.6. Post-transcriptional regulation of innate immune response

To date, lines of evidence have suggested that post-transcriptional regulation of mRNA plays a vital role in gene expression. HuR is one of the key players that binds and stabilizes target mRNA to allow persistent protein synthesis. It was suggested that HuR initially binds target mRNA inside the nucleus and remains in the messenger ribonucleoproteins (mRNPs) complex to be transported into the cytoplasm to provide ongoing protection from the degradation machinery (Fan and Steitz 1998) (Fig. 6). The untranslated mRNPs assemble as stress granule in cytoplasm, which form through interactions between RBPs that connect populations of mRNPs (Protter and Parker 2016). A previous report suggested that 44% of target mRNA screened had a HuR-binding site in both introns and 3'UTR, proposing that HuR may interact with mRNA before entering the post-

transcriptional regulatory process (Mukherjee et al. 2011). Its co-expression in common tissue localization with another RBPs protein, AUF1, brought up the possibility that HuR competes with AUF1 for the same binding area on specific mRNA target. A dynamic interaction among these two RBPs eventually determines the final cytoplasmic effect of mRNA of interest (Lal et al. 2004). Its overexpression increases the stability of ARE-containing mRNA, while possibly inhibiting mRNA decay pathway.

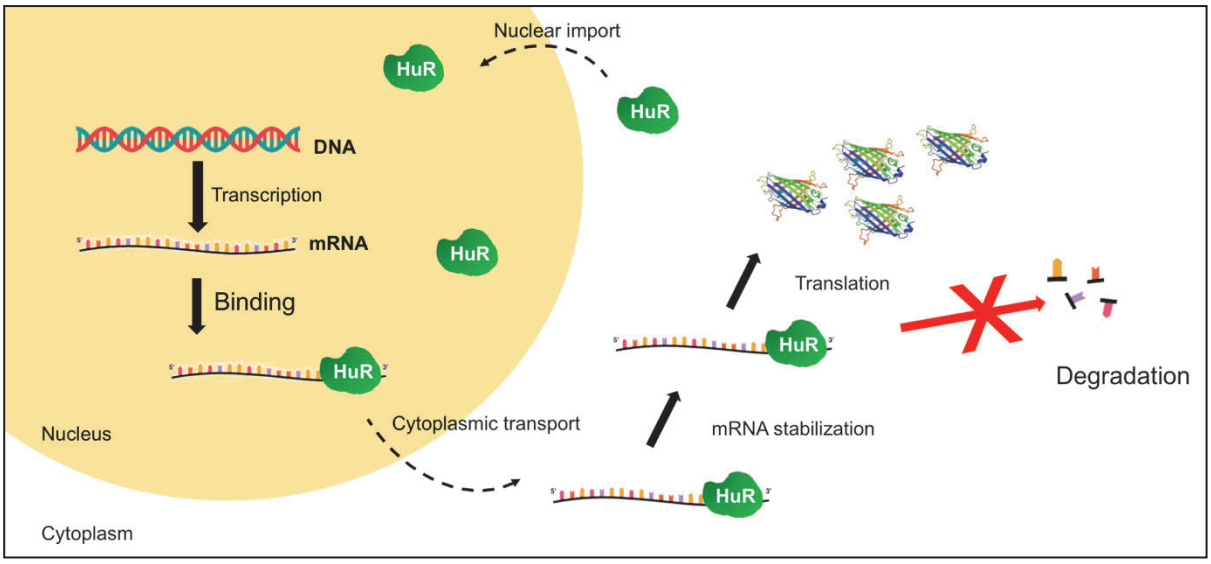


**Figure 6.** The mechanism of action of HuR on target mRNA. HuR is ubiquitously expressed in the nucleus. Upon stimulation, HuR recognizes ARE of target mRNA at their 3′UTR and form a complex. This complex is shuttled into the cytoplasmic and remain intact to allow target mRNA to be translated and remains in the cytoplasm by preventing immediate degradation.

## 1.7. Research objective

The innate immune response involves numerous transcriptional events that lead to the production of various pro-inflammatory cytokines, type I IFNs, chemokines, and secretory proteins. This response requires a proper mRNA regulatory mechanism, including post-transcriptional phase. Currently, limited literature is available on how HuR post-transcriptionally regulates innate immune responses. Hence, the present study aims to investigate the contribution of HuR on post-transcriptional regulation of genes involved in innate immunity. Our previous study showed that HuR-deficient cells exhibited reduced RLR-mediated antiviral responses. HuR regulates mRNA stabilization of Polo-like kinase 2 (PLK2), which facilitates RLR-mediated IRF3 nuclear translocation (Sueyoshi et al. 2018). I herein intended to extend the investigation on involvement of HuR in mediating innate immune response, particularly in endosomal TLRs-mediated pathways, and found that HuR is essential for TLR3-mediated signaling via the stability of *Atp6v0d2* mRNA, a component of V-ATPase.

# 2. Materials and methods

## 2.1. Cells and bacteria strain

HEK293, HEK293T and RAW264.7, and Mouse embryonic fibroblast (MEF) cells were cultured in Dulbecco's Modified Eagle's Medium (DMEM) (Nakalai Tesque) supplemented with 10% heat-inactivated fetal bovine serum (FBS) in a 5% $CO_2$ incubator. Cells were passaged using 2.5 mg/l trypsin (Nakalai Tesque) containing 10 mM Ethylenediaminetetraacetic acid (EDTA) (Nakalai Tesque).

Bacterial transformation of plasmid was conducted using *E. coli* (DH5α strain, Toyobo) cultured in LB (Luria-Bertani, Nakalai Tesque) liquid medium and grew on LB plate agar (Nakalai Tesque).

## 2.2. Generation of HuR and Atp6v0d2 Knockout cells

HuR and Atp6v0d2 knockout cells were generated as described previously (Kitai et al. 2015; Sueyoshi et al. 2018). Briefly, single guide RNA (gRNA) targeting murine *Elav1* (HuR) exon 4 (gRNA#1: 5′-GAAGACATGTTTTCTCGGTT-3′; gRNA#2: 5′-GACCATGA CACAGAAGGATG-3′) and murine *Atp6v0d2* exon 1(gRNA#1: 5′-GAAAATTCATCTCCA GACCA-3′) were inserted into pX330-U6-Chimeric_BB-CBh-hSpCas9 (Addgene). Partial fractions for both murine *Elav1* (HuR) and *Atp6v0d2* CDSs including gRNA-targeted site were inserted into pCAG-EGxxFP (Addgene). Plasmids were electroporated into RAW264.7 cells, and green fluorescent protein (EGFP)-positive cells were sorted with a FACSAria™ (BD Biosciences) and seeded onto 96-well plates. The cells were allowed to grow for two weeks before DNA was isolated and the frame-shift mutations were verified with sequence analysis (section 2.3) using following genotyping primers: forward; 5′-AGTC GAATTCGTTGGCAAGGGTTATTGCAGCCATTCTAAGAGTCTTTATC-3′, and reverse; 5′-AGTCGGATCCGAGTGCTGGGAGTAAAGGGAGGTGCCACTGTCTGTTGTGCAG

GATTTGTTTAATG-3′. The protein expression was confirmed with Western Blot (WB) following section 2.4 procedure.

## 2.3. Sequence analysis

Sequence analysis was done using BigDye™ Terminator v3.1 Cycle Sequence kit (Applied Biosystems) following manufacturer instruction. Sample preparation was performed by PCR reaction as follows:

**Table 1.** PCR set up for sequence sample preparation.

| **Reagent** | **Volume, µl** |
|---|---|
| DNA template (~100 ng/ml) | 1 |
| corresponding forward or reverse primers (1.6 pM) | 1 |
| BigDye™ Terminator v3.1 | 0.3 |
| 5x BigDye™ Terminator v3.1 reaction buffer | 2 |
| Mili Q | 5.7 |
| Total reaction | 10 |

The PCR reaction conditions were set up as follows:

**Table 2.** PCR conditions for sequence sample preparation.

| **Function** | **Temperature** | **Period** | **Number of Cycle** |
|---|---|---|---|
| Initial denaturation | 95°C | 2 Min. | 1 |
| Denaturation | 95°C | 10 Sec. | |
| Annealing | 50°C | 5 Sec. | 25 |
| Elongation | 60°C | 4 Min. | |

The PCR product (~10 μl) was subjected to ethanol sedimentation and precipitated product was dissolved with HiDi Formamide (Applied Biosystems). The resulting DNA solution was heat-treated at 95°C. for 5 minutes, and nucleotide sequence data were obtained using a capillary sequencer (Applied Biosystems 3130 × L Genetic Analyzer). The nucleotides sequence was then examined using GENETYX ver. 12.

**Table 3.** Primers for sequence analysis for this study.

| **Primer** | **Sequence (5′-3′)** | **Target** |
|---|---|---|
| pFlagCMV_sequnece_forward | CGCAAATGGGCGGTAGGCGTG | pFlag-CMV-2 |
| pFlagCMV_sequnece_reverce | GCACTGGAGTGGCAACTTCC | pFlag-CMV-2 |
| px330_sequence_forward | TGGACTATCATATGCTTACC | px330 |
| pCAG-EGxxFP_sequence_forward | GCCTTCTTCTTTTTCCTACAGC | pCAG-EGxxFP |
| pGL3promoter_Xba1_sequence | CGTGGATTACGTCGCCAGTCAAG | pGL3-promoter |
| M13_Reverse_primer | CAGGAAACAGCTATGAC | TOPO |

## 2.4. Western blot

Cells were seeded on 6-wells plates and stimulated with 50 μg/ml poly(I:C) for 8 hours. Cells were lysed with 150 μl of RIPA buffer (50 mM Tris-HCl, pH 8, 150 mM NaCl, 0.1% SDS, 0.5% sodium deoxycholate, 1% Nonidet P-40). The whole-cell lysates (supernatant) collected from centrifugation at 3,000 rpm, 4°C for 10 minutes were subjected to 4X SDS-PAGE (0.125 M Tris-HCl, 4% SDS, 20% Glycerol, 0.01% Bromophenol blue, 0.2 M dithiothreitol) and heated at 95°C for 5 minutes. Samples were electrophoresed through 1.0 mm 10% acrylamide gel using TGX$^{TM}$ FastCast$^{TM}$ Kit (Bio-Rad Laboratories) in SDS-PAGE Running buffer (0.25 M Tris, 1% SDS, 1.92 M Glycine) at 20 mA for 90 minutes.

The separated proteins were transferred to Immun-Blot PVDF membrane (Bio-Rad Laboratories) in transfer buffer (25 mM Tris, 20% methanol, 1.92 mM Glycine) at 200 mA for 70 minutes, in the cool room (4°C). The membrane was then blocked by incubating the membrane in blocking solution containing 5% skim milk in TBST buffer (20mM M Tris, pH 7.6, 150 mM NaCl, 0.1% tween 20) for 1 hour at room temperature. The membrane was washed with TBST and immunoblotted with the indicated primary antibodies (Table 4) in blocking solution, overnight at 4 ° C. Following day: the membrane was washed again before incubated with secondary antibody (Table 4) in blocking solution at room temperature for 30 minutes. After the final wash, the membrane was exposed with Western Lightning Plus-ECL (PerkinElmer) under LAS 4000 (Fujitsu Life Sciences).

**Table 4.** Antibodies and their respective dilution factors used in immunoblot.

| **Antibody** | **Supplier** | **Dilution factor** |
|---|---|---|
| **Primary** | | |
| anti-HuR mouse monoclonal antibody (3A2) | Santa Cruz | 1/1,000 |
| anti-Actin goat polyclonal antibody (I-19) | Santa Cruz | 1/1,000 |
| anti-IRF3 rabbit monoclonal antibody (D83B9) | Cell Signaling Technology | 1/1,000 |
| anti-Phospho-IRF3 (Ser396) rabbit monoclonal antibody (4D4G) | Cell Signaling Technology | 1/1,000 |
| anti-TOM20 rabbit polyclonal antibody (FL-145) | Santa Cruz | 1/1,000 |
| **Secondary** | | |
| HRP-conjugated anti-Mouse IgG monoclonal antibody | Sigma | 1/30,000 |
| HRP-conjugated anti-Goat IgG monoclonal antibody | Sigma | 1/30,000 |
| HRP-conjugated anti-rabbit IgG monoclonal antibody | Sigma | 1/30,000 |

## 2.5. Plasmid construction

The full-length mouse *Elav1* (HuR), and *Atp6v0d2* coding sequences (CDS) were constructed using primers as follows:

**Table 5.** Primers used for construction of expression plasmid.

| **Primer** | **Sequence (5′-3′)** | **Restriction enzyme** |
|---|---|---|
| pFLAGCMV_HuR_fwd | ATGGGAATTCTATGTCTAATGGTTATGAAGA | *EcoR* I |
| pFLAGCMV_HuR_rev | ATCGTCGAGTTATTTGTGGGACTTGTTGGT | *Sal* I |
| pFLAGCMV_v0d2_fwd | ATGCAAGCTTATGCTTGAGACTGCAGAGCTGTAC | *Hind*Ⅲ |
| pFLAGCMV_v0d2_rev | ATGCGAATTCTAAAATTGGAATGTAGCTGTTGATTTTAG | *EcoR* I |

PCR reactions were performed using murine brain and lung cDNA, respectively, using the following set up:

**Table 6.** PCR set up for plasmid construction.

| **Reagent** | **Volume, μl** |
|---|---|
| Mouse DNA template (~100 ng/ml) | 1 |
| corresponding forward or reverse primers (1.5 pM) | 1, each |
| KOD FX (TOYOBO) | 0.5 |
| 2 × FX Buffer (TOYOBO) | 12.5 |
| dNTPs Mix (TOYOBO) | 5 |
| Mili Q | 4 |
| Total reaction | 25 |

The PCR reaction conditions were set up as follows:

**Table 7.** PCR condition for plasmid construction.

| Function | Temperature | Period | Number of Cycle |
|---|---|---|---|
| Initial denaturation | 98°C | 2 Min. | 1 |
| Denaturation | 98°C | 30 Sec. | |
| Annealing | 50°C | 30 Sec. | 25 |
| Elongation | 72°C | 5 Min. | |
| Final extension | 72°C | 8 Min. | 1 |

The resulting amplification products were purified using a DNA purification kit (GE Healthcare) and treated with respective restriction enzymes (TOYOBO) for 1 hour at 37°C. After purification, the enzyme-treated amplification product was inserted into enzyme-treated pFLAG-CMV-2 expression vector (Sigma-Aldrich) via ligation process at 16°C, for 4 hours in 2x ligation mix (TOYOBO). The ligation product was transformed into *E. coli* DH5α strain (TOYOBO) by briefly heated the cell mixture at 42°C for 1 minute, and immediately smeared onto LB agar medium and allow to grow at 37°C overnight. Following days, the colonies obtained were inoculated into LB broth containing 50 μg/ml ampicillin and left overnight at 37°C. The overnight inoculated broth was then used to extract plasmid using FastGene Plasmid Mini Kit (NIPPON Genetics). The sequence of the gene was confirmed by sequence analysis as in section 2.3.

The series of mutants for HuR expression plasmids (Fig. 7) were generated by PCR from the original full-length HuR-expressing pFLAG-CMV-2 vector. Primers used to generate the mutants were presented in table 8. After amplification by PCR using KOD FX reaction (followed Tables 6 and 7 protocols), the amplification product was purified and treated with *Dpn*l restriction enzyme to remove *E.coli*-derived template. Re-purified product was transformed into *E. coli* DH5α strain and extracted accordingly.

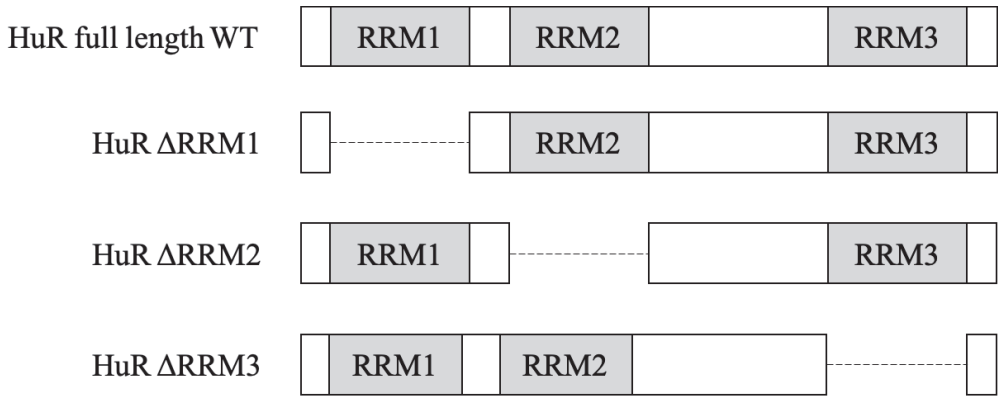


**Figure 7.** Schematic structure of the pGL3 vector containing the full-length HuR cDNA sequence or its domain deletion mutants (ΔRRM1, ΔRRM2, and ΔRRM3).

**Table 8.** Primers used to construct domain-deficient HuR

| **Primer** | **Sequence (5′-3′)** |
|---|---|
| pFLAGHuR_ΔRRM1_fwd | ATTGGGAGAACGAATGTGTCATATGCTCGCCCAAGCTCAG |
| pFLAGHuR_ΔRRM1_rev | ATTCGTTCTCCCAATGTCATCCC |
| pFLAGHuR_ΔRRM2_fwd | ATCAAAGATGCCAACGAGCCCATCACAGTGAAGTTTGC |
| pFLAGHuR_ΔRRM2_rev | GTTGGCATCTTTGATGACCTC |
| pFLAGHuR_ΔRRM3_fwd | TCCTCGGGCTGGTGCGTTTCCTTCAAAACCAACAAG |
| pFLAGHuR_ΔRRM3_rev | GCACCAGCCCGAGGAAGCATTGCCG |

The pGL3 (Promega) harbouring the mouse *Atp6v0d2* 3′UTR (pGL3-*Atp6v0d2*-3′UTR) was constructed (Fig.8) with the PCR amplification of the mouse *Atp6v0d2* 3′UTR sequence from murine thymus cDNA, using forward primer; 5-GCCGTGTAATTCTAGACTCACAG AGGCATCGAACTA-3′, and reverse primer; 3′-CCGCCCCGACTCTAGAGGCAATCCCA AAATCAAGTT-5′. The purified product was inserted into *Xba*I-digested pGL3 vector, transformed, and extracted accordingly. Deletion mutants for pGL3-*Atp6v0d2*-3′UTR were generated by site-directed mutagenesis using the primers as listed in table 9. The reporter plasmids for IFN-β was constructed as described previously (Kitai et al. 2015; Sueyoshi et al. 2018).

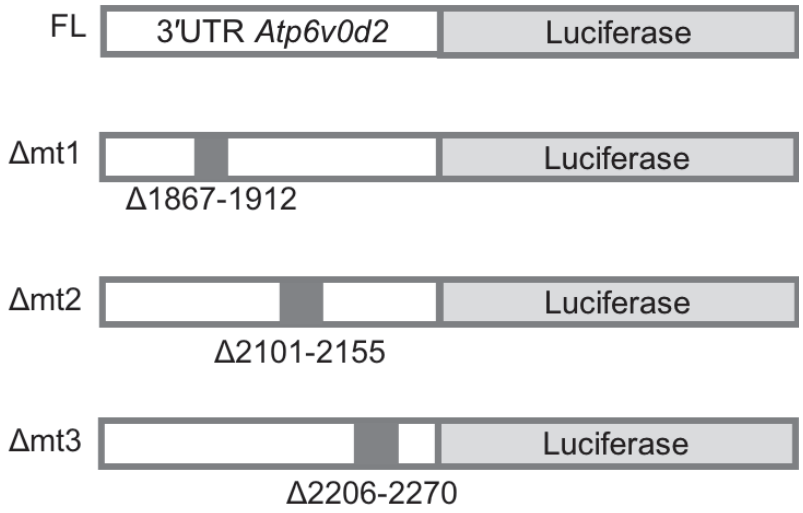


**Figure 8.** Schematic structure of the pGL3 vector containing the full-length 3′UTR of *Atp6v0d2* (FL) or its deletion mutants (Δmt1, Δmt2, or Δmt3).

**Table 9.** Primers used to construct *Atp6v0d2* 3'UTR deletion mutants.

| **Primer** | **Sequence (5′-3′)** |
|---|---|
| pGL3v0d2_Δmt1_fwd | TCTATGCTTGCTCTGCTTCAC |
| pGL3v0d2_Δmt1_rev | ATTTTGCTATTTTTCTTTTTCTGAGCAACCTC |
| pGL3v0d2_Δmt2_fwd | ACTCTCTATATACACATGCTATGTAGAATAGTATGC |
| pGL3v0d2_Δmt2_rev | AGTGTGTGTAGTGGTGGGGT |
| pGL3v0d2_Δmt3_fwd | AGAAAGCCAAGTGCCTACTC |
| pGL3v0d2_Δmt3_rev | GCTCCTTAGTTTATGCATACTATTCTACATAGC |

## 2.6. Acridine orange staining

Approximately 1 X $10^6$ of RAW264.7 and HuR knockout cells were seeded in 35 mm glass-bottom culture dish (MatTek) overnight. After the medium was removed, the cells were carefully washed with cold PBS before incubated with freshly prepared 5 μg/ml acridine orange solution for 5 minutes. For negative control, cells were treated with 10 nM Bafilomycin A1 1 hour prior to acridine orange treatment. The staining solution was then replaced with free RPMI medium after washing for immediate observation under microscope.

The cells were excited at 488 nm and emission was detected at 520 nm (green; 520 nm) for the internal marker and 620 nm for endosomal acidification (red; 620 nm) by confocal microscopy LSM 700 (Carl Zeiss). Images were corrected within an hour of acridine orange treatment.

## 2.7. Inhibition of endosomal acidifications

RAW246.7 cells seeded on 24-wells plate were treated with different concentration of Bafilomycin A1 an hour prior to poly(I:C) stimulation. After 8 hours of poly(I:C) stimulation, total RNA was extracted using TRIzol reagent. RT-qPCR was performed to measure the expression of mRNA expression level.

## 2.8. Immunofluorescence staining

Coverslip was coated with the poly-L-lysine solution (Sigma) in 24 wells culture plate. After UV sterilization, RAW264.7 cells were seeded onto the coverslip. Cells were stimulated with 50 μg/ml poly(I:C) for 8 hours and washed with PBS before fixed in 4% paraformaldehyde in PBS (Nakalai Tesque) for 20 minutes at room temperature. The cells on the coverslip than were washed with 0.02% triton in PBS before incubated with 100 mM glycine in 0.02% triton PBS for 30 minutes at room temperature. After washing, the cells were incubated with a blocking solution containing 10% FBS in 0.02% triton PBS at 4°C, overnight. Thereafter, the cells were treated overnight with the primary antibody in blocking solution, at 4°C. After washing, the cells were incubated with secondary antibody in blocking solution for one hour at 37°C in the dark. The cells were washed and incubated with nucleus staining (Hoechst 33342) for 10 minutes in the dark at room temperature before washed and sealed onto a glass slide using Fluoro-KEEPER Antifade Reagent (Nakalai Tesque). The slide was then observed under confocal fluorescence microscope LSM 700 (ZEISS), and the

image obtained was processed by ZEN software. The dilution factors of antibodies used were listed in the following table:

**Table 10.** Dilution factors of antibodies used in immunofluorescence microscopy.

| Antibody | Supplier | Dilution factor |
|---|---|---|
| **Primary** | | |
| anti-HuR mouse monoclonal antibody (3A2) | Santa Cruz | 1/100 |
| anti-G3BP rabbit polyclonal antibody | Sigma | 1/100 |
| **Secondary** | | |
| Alexa Fluor 488 rabbit anti-Mouse IgG (H+L) Cross-Adsorbed Secondary Antibody | Invitrogen | 1/30,000 |
| Alexa Fluor 568 mouse anti-Rabbit IgG (H+L) Cross-Adsorbed Secondary Antibody | Invitrogen | 1/30,000 |

## 2.9. HuR knockdown cells

shRNAs were introduced into the *Bgl*II and *Hin*dIII sites of the retroviral vector pSUPER.retro.Puro (OligoEngine), as previously described (Sueyoshi et al. 2018). The oligonucleotide sequences used were: scrambled shRNA, 5′-CCTAAGGCTATGAAGAGAT ACTTCAAGAGAGTATCTCTTCATAGCCTTATTTTT-3′; and HuR shRNA, 5′-GAGAAC GAATTTAATTGTCAACTTTCAAGAGAAGTTGACAATTAAATTCGTTCTC-3′.

Platinum-E cells were transfected with the shRNA-carrying vectors with Lipofectamine 2000 (Life Technologies) and Opti-MEM medium (Life Technologies) in a ratio of 1:1 (μg/μl). After 6 hours post-transfection, the medium was changed to fresh DMEM and cultured for two days. The supernatant was filtered through a 0.22 μm Millex-GV Filter Unit (Merck Millipore) and incubated with RAW264.7 and MEF cell. The cells were selected with 2 μg/ml puromycin (Invivogen) for 48 hours, and the surviving cells were used for the

subsequent experiments. The confirmation of protein knockdown was done by WB as described in section 2.4.

## 2.10. RNA isolation and cDNA synthesis

Cells were seeded in 24-wells plates and stimulated with 50 μg/ml LMW poly(I:C) for 8 hours. Cells were washed with cold PBS, and total RNA extraction was performed using 500 μl TRIzol reagent (Molecular Research Center, Inc.) per well. The volume of 100 μl chloroform was added to the TRIzol-cell mixture, vortex thoroughly, and centrifuged at 14,000 rpm for 10 minutes at 4°C. Next, 500 μl of isopropanol (Nacalai Tesque) was added to the collected supernatant and centrifuged at 14,000 rpm for 15 minutes at 4°C. A volume of 800 μl of 70% ethanol was added to the supernatant, and centrifuged at 14,000 rpm, 4°C, for 5 minutes. The ethanol was discarded, and the pellet was washed again with 500 μl of 70% ethanol under the same centrifugation steps. The ethanol was then completely removed by pre-heated with heat block at 37°C. The pallet was dissolved 15 μl Diethyl pyrocarbonate (DEPC)-treated sterile water [0.1% DEPC] to obtain total RNA, and the concentration was measured using NanoDrop One/OneC (Thermo Fisher Scientific). By using 0.5 to 1 μg of RNA as a template (based on final RNA concentration), cDNA was synthesized using ReverTraAce (TOYOBO) reaction kit according to the manufacturer's protocol.

**Table 11.** PCR set up for cDNA synthesis.

| Reagent | Volume, µl |
|---|---|
| RNA template (~50 ng/ml) | 0.5 to 1 |
| Random primer | 0.5 |
| dNTPs | 1 |
| ReverTraAce (TOYOBO) | 0.5 |
| ReverTraAce buffer (TOYOBO) | 2 |
| Mili Q (depend on RNA template used) | 5-5.5 |
| Total reaction | 10 |

**Table 12.** Heat treatment condition for cDNA synthesis.

| Function | Temperature | Period | Number of Cycle |
|---|---|---|---|
| Denaturation | 30°C | 10 Min. | 1 |
| Annealing/extension | 42°C | 60 Min. | 1 |
| Final extension | 99°C | 5 Min. | 1 |

## 2.11. Real-time quantitative PCR

Following cDNA synthesis (section 2.10), the samples were subjected to real-time quantitative PCR (RT-qPCR) using Power SYBR Green PCR Master Mix (Applied Biosystems). A volume of 20 µl reaction solution was prepared according to the manufacturer's protocol (table 13). The primers used are as listed in table 14. The m*Gapdh* gene was used as an internal control gene.

**Table 13.** Reaction set up for RT-qPCR.

| **Reagent** | **Volume, µl** |
|---|---|
| cDNA template | 4 |
| Primers: forward + reverse | 0.15 + 0.15 |
| 2X Power SYBR Green PCR Master Mix | 10 |
| Mili Q | 5.7 |
| Total reaction | 20 |

**Table 14.** Primers used in RT-qPCR reaction.

| **Gene** | **Species** | **Primer sequence (5′-3′)** |
|---|---|---|
| m*HuR*_F | Mouse | ATGAAGACCACATGGCCGAAGACT |
| m*HuR*_R | Mouse | AGTTCACAAAGCCATAGCCCAAGC |
| m*Atp6v0d2*_F | Mouse | TCAGATCTCTTCAAGGCTGTGCTG |
| m*Atp6v0d2*_R | Mouse | GTGCCAAATGAGTTCAGAGTGATG |
| *Ifnb1*_F | Mouse | ATGGTGGTCCGAGCAGAGAT |
| *Ifnb1*_R | Mouse | CCACCACTCATTCTGAGGCA |
| *Cxcl10*_F | Mouse | CCTGCAGGATGATGGTCAAG |
| *Cxcl10*_R | Mouse | GAATTCTTGTTCGGCAGTT |
| m*Gapdh*_F | Mouse | TGACGTGCCGCCTGGAGAAA |
| m*Gapdh*_R | Mouse | AGTGTAGCCCAAGATGCCCTTCAG |
| h*ATP6V0D2*_F | Human | CTTGAGTTTGAGGCCGACAG |
| h*ATP6V0D2*_R | Human | TGCCGAAGGTTGGATAGAGG |
| h*GAPDH*_F | Human | AATCCCATCACCATCTTCCA |
| h*GAPDH*_R | Human | TGGACTCCACGACGTACTCA |

The measurement was conducted using the Light Cycler 96 system (Roche Diagnostics). The relative amount of mRNA in the sample was evaluated using the ΔCt method accordingly.

**Table 15.** One-step protocol for heat treatment of RT-qPCR used.

| Temperature | Period | Number of Cycle |
|---|---|---|
| 95°C | 10 Min. | 1 |
| 95°C | 10 Sec. | 50 |
| 60°C | 1 Min. | 1 |

## 2.12. Luciferase reporter assay

HEK293T cells were seeded on 24-wells plates and transiently transfected with 100 ng of a reporter plasmid containing *IFN-β* promoter, *Atp6v0d2* 3′UTR or one of the constructed *Atp6v0d2* 3′UTR deletion mutants together with 500 ng of HuR expression plasmid or empty plasmid. Internal control used was 10 ng pRL-TK (Promega), which was transfected simultaneously. Alternatively, HuR domain deletion mutants were co-transfected with full-length *Atp6v0d2* 3′UTR together with internal control plasmid. The medium was replaced after 6 hours, and after 24 hours post-transfection, the luciferase activity was measured with TriStar$^2$ LB 942 Multidetection Microplate Reader (Berthold) using Dual-Glo Luciferase System (Promega). The targeted genes promoter activity is normalized by Renilla Luciferase for transfection efficiency.

## 2.13. RNA immunoprecipitation

Ab-conjugated protein-A Sepharose beads (GE Healthcare) were prepared by washing NT2 buffer (50 mM Tris-HCl, pH 7.4, 1 mM $MgCl_2$, 150 mM NaCl, and 0.05% Nonidet P-40). The beads were incubated with NT2 buffer supplemented with 5% BSA at 4°C for 2 hours. After washing with NT2 buffer, the beads slurry was divided into two parts and incubated with either control IgG or anti-HuR antibody at 4°C with constant agitation overnight. RAW264.7 cells were plated in 6-wells plate and were stimulated with 50 μg/ml poly(I:C). After 8 hours' stimulation, the cells were washed with PBS and were suspended in polysome lysis buffer [100 mM KCl, 5 mM $MgCl_2$, 0.5% Nonidet P-40, 10 mM HEPES, pH 7, 1 mM Dithiothreitol (DTT), RNaseOut (Invitrogen) and Protease inhibitors cocktail]. The cells were collected and lysed by 26G syringe needle (Terumo). After centrifugation at 15,300 X g at 4°C for 15 minutes, the supernatants were incubated with Ab-conjugated beads for 2 hours at room temperature with constant agitation. The Ab-conjugated beads were first washed with NT2 buffer for five times and were treated with TRIzol reagent for RNA extraction. RT-qPCR was conducted to measure the expression of *Atp6v0d2* mRNA level.

## 2.14. mRNA degradation rate

Twenty-four-wells plates were seeded with HEK293T cells and transiently transfected with 500 ng of the pFlag-CMV2-HuR plasmid. LMW poly(I:C) (50 μg/ml) stimulation was performed for 8 hours before the transcription inhibitor actinomycin D (Sigma) was added to at the concentration of 5 μg/ml. Every hour after the treatments, cells were harvest using TRIzol reagent, and the total RNA extraction was conducted as described above. After calculating the target mRNA abundance under control conditions by the ΔCt method, the

value was set to 100, and the relative amount of target mRNA abundance at each time point after actinomycin treatment was calculated. The calculated values were plotted on a scatter plot, an approximate curve was extrapolated, and the half-life ($t^{1/2}$) was calculated based on the displayed equation. Alternatively, RAW 264.7 control and HuR KO cells were treated with 30 minutes interval following the stimulation and actinomycin D treatment and were harvested at indicated time points.

# 3. Result

## 3.1. HuR knockout (KO) reduces poly(I:C)-induced immune responses

Our laboratory previously demonstrated that HuR KO murine macrophage cells (RAW264.7 cells) showed reduced RLR-mediated nuclear translocation of IRF3 and reduced *Ifnb1* expression (Sueyoshi et al. 2018). Therefore, I used these KO cells to test innate immune responses to endosome-localized TLRs such as TLR3, TLR7, and TLR9. Initially, the defective expression of HuR protein in two HuR KO cell lines (KO1, KO2) was confirmed with western blotting (WB) (Fig. 9a). I then stimulated these cells with poly(I:C) for 8 hours and measured their *Ifnb1* and *Cxcl10* mRNA expression with RT-qPCR, and found that *Ifnb1* and *Cxcl10* mRNA expression was significantly reduced in HuR KO cells after poly(I:C) stimulation relative to that in wild-type (WT) cells (Fig. 9b). Next, I stimulated WT and HuR KO1 cells with R837 and ODN1668, a synthetic ligand for TLR7 and TLR9, respectively, in addition to poly(I:C), and found that these cytokines expression was unimpaired in HuR KO1 cells after R837 or ODN1668 stimulation (Fig. 9c). WB analysis indicated that the phosphorylation of IRF3 was lower after poly(I:C) stimulation in HuR KO1 cells than in WT cells (Fig. 9d). Thus, these results suggest that HuR is required for IRF3 activation by TLR3 but not TLR7 and TLR9.

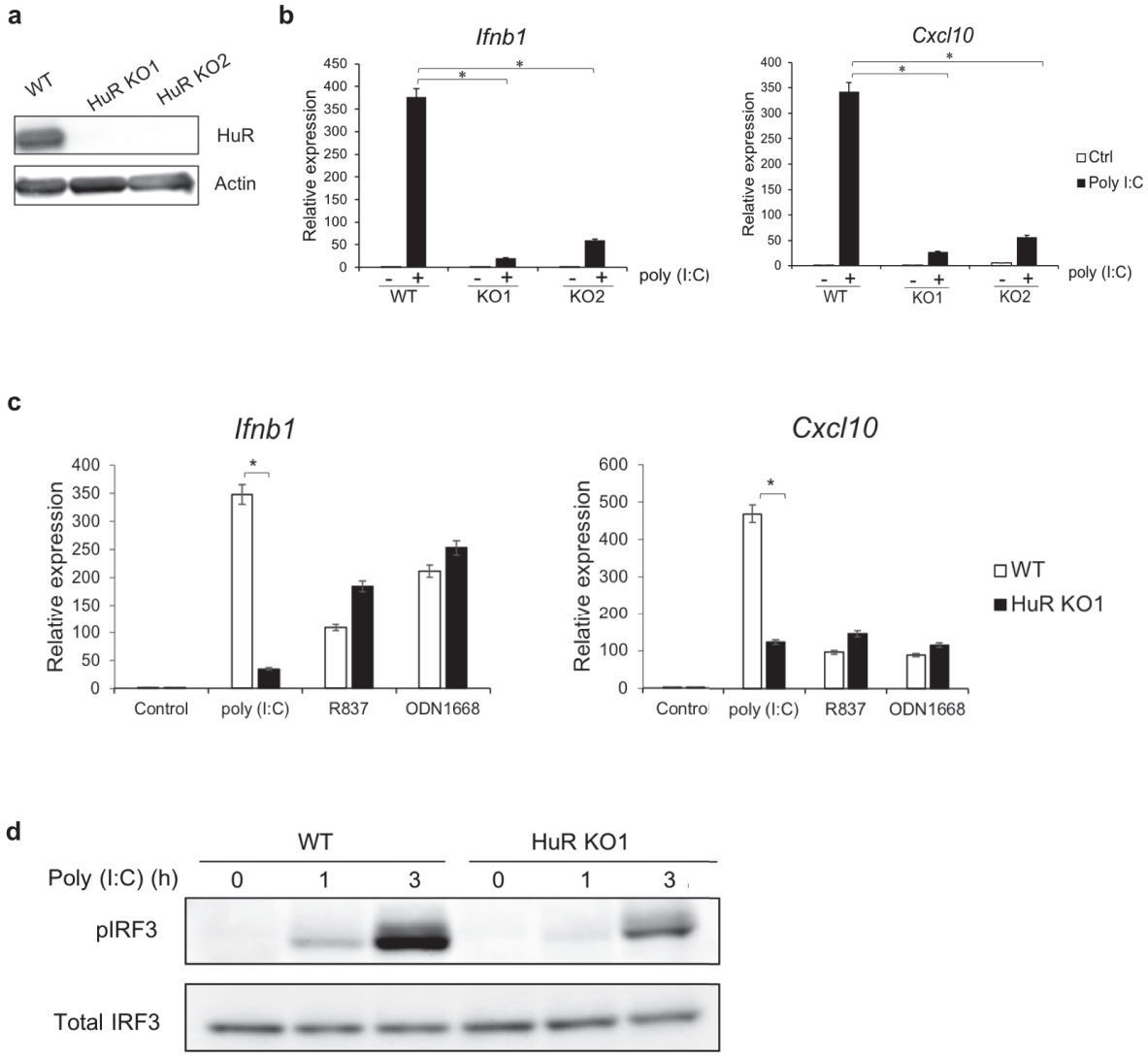


**Figure 9.** Reduced poly(I:C)-induced immune response in HuR KO cells. (**a**) cell lysates from WT, HuR KO1, and HuR KO2 cells were subjected to western blot (WB) using indicated antibodies. (**b**) WT, HuR KO1, and HuR KO2 cells were stimulated with poly(I:C) for 8 hours before the expression level of *Ifnb1* and *Cxcl10* mRNA were quantitate with RT-qPCR. (**c**) WT and HuR KO1 cells were stimulated with R837 and ODN1668, and Ifnb1 and Cxcl10 mRNA expression were measured with RT–qPCR. (**d**) WT and HuR KO1 cells were stimulated with poly(I:C) for the indicated times, and the cell lysates were subjected to WB and probed with an anti-pIRF3 or anti-IRF3 antibody. Data are the means ± SE of triplicate independent experiments. *$p < 0.01$, Student's t-test.

To examine the ability of exogenous HuR to restore the response of TLR3 in HuR KO cells, I expressed FLAG-HuR into HuR KO1 cells via retrovirus transfer system. FLAG–HuR expression was confirmed with WB against anti-FLAG and anti-HuR antibodies (Fig. 10a). Exogenous FLAG–HuR restored the expression of *Ifnb1* and *Cxcl10* mRNA after poly(I:C) stimulation to a level similar to that in the WT cells (Fig. 10b).

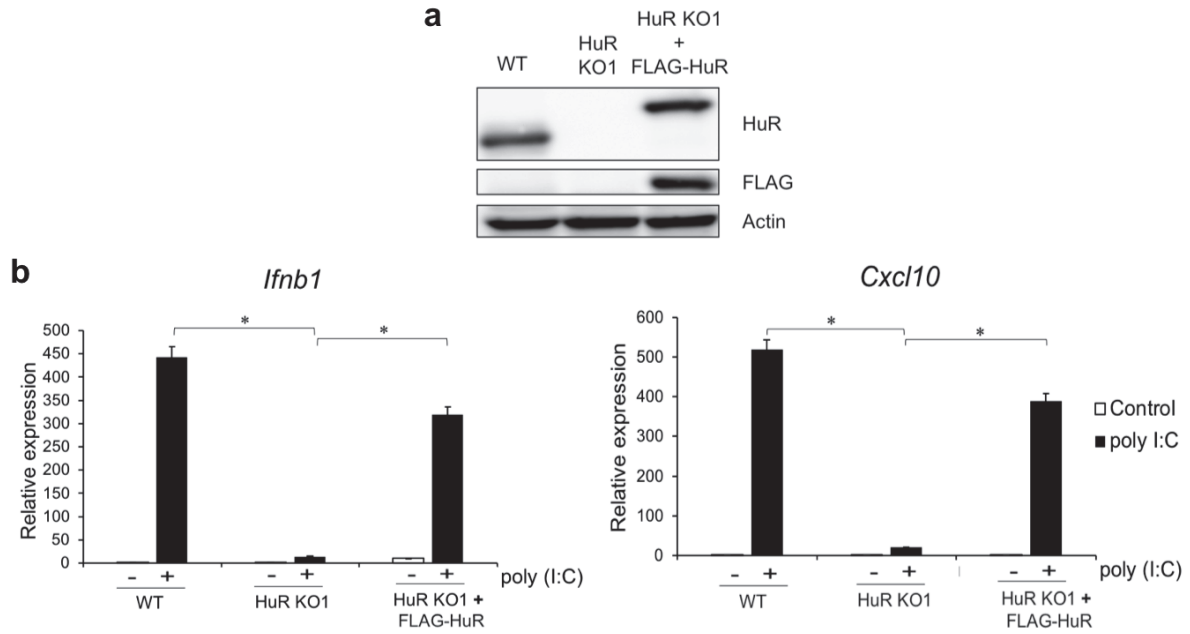


**Figure 10.** Exogenous HuR restores TLR3 immune response in HuR KO cells. (**a**) the FLAG-HuR-expressing plasmid was stably transfected into HuR KO cells. The lysates of WT, HUR KO1, and transfected HuR KO1 cells were analyzed by WB and probed with indicated antibodies. (**b**) These cells were then stimulated with poly(I:C) and the expression levels of *Ifnb1* and *Cxcl10* mRNAs were measured with RT–qPCR. Data are the means ± SE of triplicate independent experiments. *$p < 0.01$, Student's t-test.

### 3.2. HuR knockdown reduces TLR3-mediated innate immune responses

To evaluate the effects of HuR protein in other cell types, I knocked down its expression in mouse embryonic fibroblasts (MEFs). MEF cells were treated with scrambled or HuR-directed small hairpin RNA (shRNA), and the reduced HuR expression was confirmed by WB with an anti-HuR antibody (Fig. 11a) and RT–qPCR (Fig. 11b). In the HuR knockdown cells, *Ifnb1* and *Cxcl10* mRNA expression after poly(I:C) stimulation was significantly reduced compared with that in the control cells (Fig. 11c).

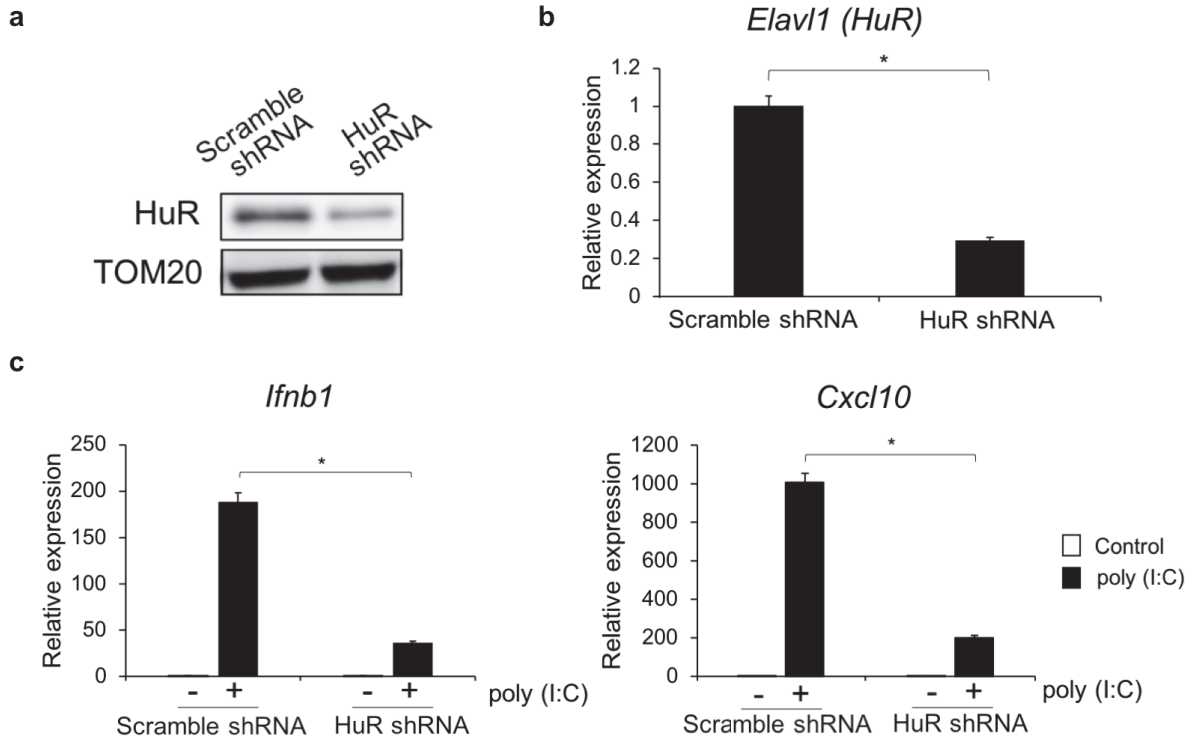


**Figure 11.** Knockdown of HuR gene reduces TLR3-mediated immune response. MEF cells were infected with a retrovirus expressing scrambled or HuR-directed shRNA and were selected with puromycin. Expression of HuR was confirmed with western blotting (WB) (**a**) and RT-qPCR (**b**). MEF cells were stimulated with poly(I:C) before expression level of *Ifnb1* and *Cxcl10* was quantified with RT–qPCR (**c**). Data are the means ± SE of triplicate independent experiments. *p < 0.01, Student's t-test.

I also knocked down HuR in RAW264.7 cells and confirmed HuR expression by WB and RT-qPCR (Fig. 12a, b), and found that HuR knockdown caused a significant reduction in *Ifnb1* and *Cxcl10* mRNA after poly(I:C) stimulation compared with scrambled shRNA (Fig. 12c). These results supported that HuR is required for the innate immune response to poly(I:C).

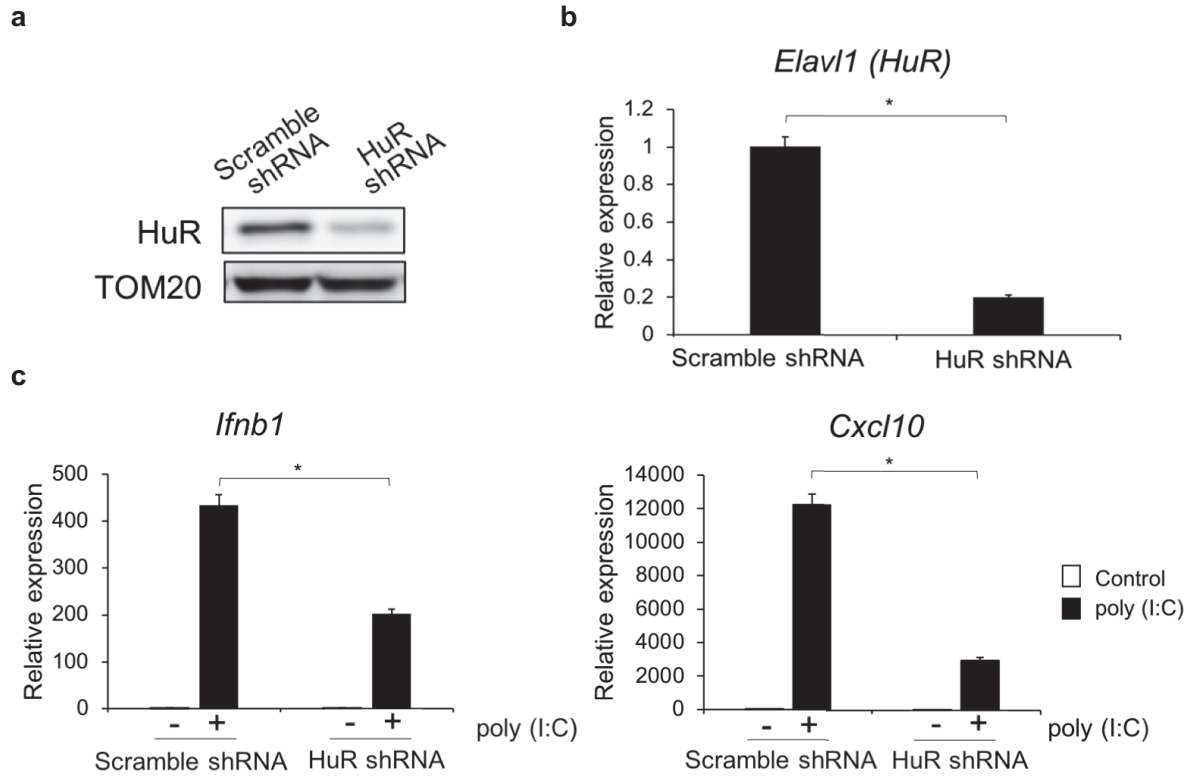


**Figure 12.** RAW264.7 cells were infected with a retrovirus expressing scrambled or HuR-directed shRNA and were selected with puromycin. Expression of HuR in cells was confirmed with western blotting (WB) (**a**) and RT-qPCR (**b**). RAW264.7 cells were stimulated with poly(I:C) before expression level of *Ifnb1* and *Cxcl10* was quantified with RT–qPCR (**c**). Data are the means ± SE of triplicate independent experiments. *$p < 0.01$, Student's t-test.

### 3.3. HuR localization in RAW264.7 cells

It is generally known that stress granules (SGs) are the subset of RBPs and mRNA assembly site during cellular stress. SGs interfere with mRNA degradation, which in turn promote mRNA stabilization under stress. Its formation is induced by cellular stress response, viral infection, and various signaling pathways (Protter and Parker 2016). RBPs such as HuR was reported to mobilize from nuclei to SGs during stress condition, and associate with G3BP. Thus, their co-localization represents that the cells are under stress (Bley et al. 2015). To address if HuR translocates to SGs upon poly(I:C) stimulation, I stained RAW264.7 cells with anti-HuR and anti-G3BP antibodies (Fig. 13). Unstimulated cells showed the nuclear localization of HuR (green) whilst HuR underwent cytoplasmic translocation which partially co-localized with G3BP (red) after stimulation with poly(I:C). These results suggest that HuR mobilizes to cytoplasmic stress granule from nuclei upon poly(I:C) stimulation.

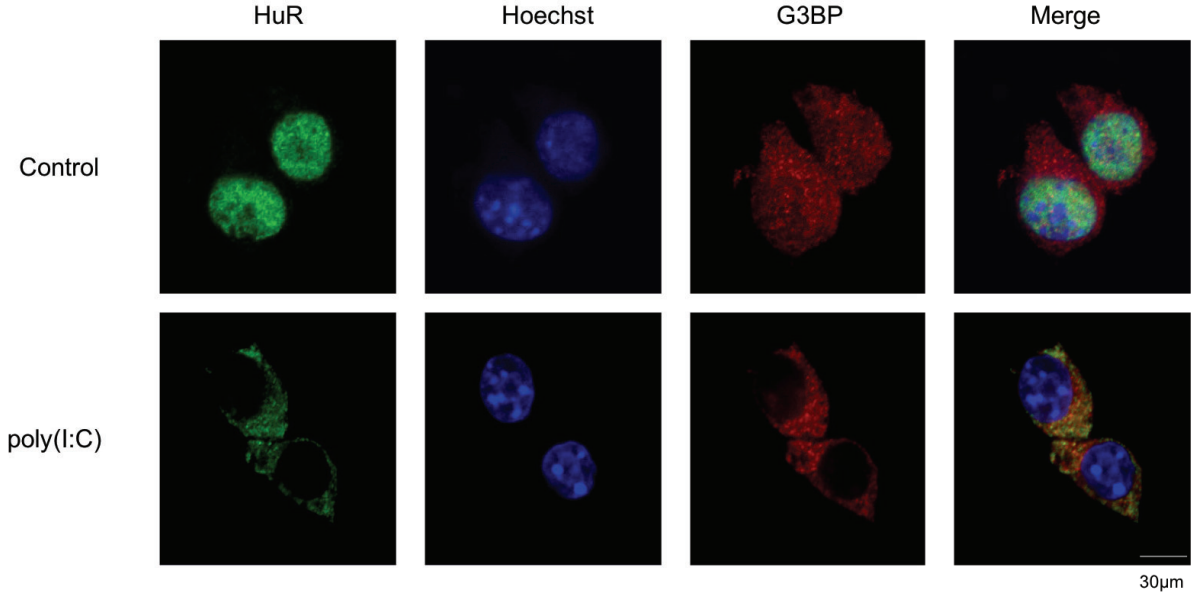


**Figure 13.** Subcellular localization of HuR upon poly(I:C) stimulation. HuR, tagged with green fluorescence protein (GFP) localizes in the nucleus at resting state (upper panels). Upon 8 hours poly(I:C) stimulation, HuR translocates to the cytoplasmic aggregates in part with the stress granules indicated by the red-fluorescence signal of G3BP marker (lower panels). Blue signals were nuclear stain (Hoechst).

### 3.4. *Atp6v0d2* mRNA is regulated by HuR

HuR is shown to associate with the 3′UTR of its target mRNAs to maintain their stability (Brennan and Steitz 2001), so HuR deficiency is expected to reduce the expression of the target mRNAs. Our laboratory previously showed that the expression levels of TLR3 signaling molecules, including TRIF and IRF3 was unaltered by HuR deficiency (Sueyoshi et al. 2018), but we subsequently found that *Atp6v0d2* was reduced in HuR KO cells. I therefore measured again the expression of *Atp6v0d2* mRNA in WT and HuR KO RAW264.7 cells stimulated with or without poly(I:C). In WT cells, the expression of *Atp6v0d2* mRNA increased after stimulation with poly(I:C). However, *Atpv60d2* mRNA expression in the steady-state was lower in HuR KO cells than in WT cells, and its expression after poly(I:C) stimulation was markedly reduced in HuR KO cells (Fig. 14a). In contrast, the mRNA levels of other V-ATPases subunit genes, such as *Atp6v1a* and *Atp6v1b2*, showed no significant reduction in HuR KO cells (Fig. 14b, c). The expression of *Atp6v0d2* mRNA was also complemented by FLAG–HuR expression in HuR KO cells (Fig. 14d). Altogether, these results suggest that *Atp6v0d2* mRNA expression is maintained by HuR.

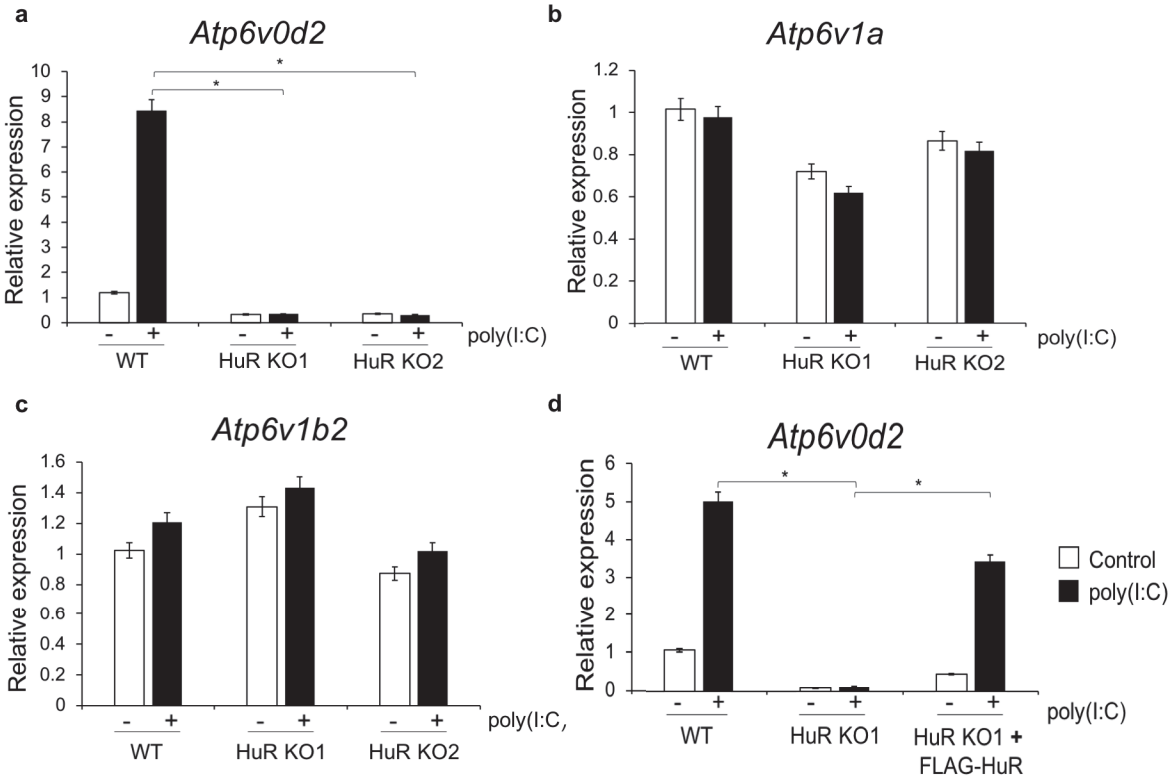


**Figure 14.** HuR regulates *Atp6v0d2* mRNA expression level. HuR KO1 and KO2 cells were stimulated with poly(I:C) and the levels of mRNA of selected V-ATPases namely *Atp6v0d2* (**a**), *Atp6v1a* (**b**), and *Atp6v1b2* (**c**) were measured via RT-qPCR. (**d**) HuR KO1 cells stably expressed FLAG–HuR after retroviral infection. Wild-type (WT), HuR KO1, and HuR KO1+FLAG–HuR cells were stimulated with poly(I:C) and *Atp6v0d2* mRNA expression was measured with RT–qPCR. Data are the means ± SE of triplicate independent experiments. *p < 0.01, Student's t-test.

## 3.5. HuR deficiency disrupts endosomal acidification

It is well established that the acidic condition is crucial for endosomal TLRs activation. So, I examined the effect of an immune response upon inhibition of endosomal acidification using a potent ATPase inhibitor, Bafilomycin A1. Treatment with Bafilomycin A1 prior to poly(I:C) stimulation demonstrated a significant reduction in *Ifnb1* and *Cxcl10* expression as compared to untreated cells, hence, confirmed the disruption of endosomal acidification which is likely linked to poly(I:C)-mediated response (Fig. 15a). V-ATPase is known to maintain the acidification of the endosome by proton transport. Therefore, I

evaluated the effect of HuR deficiency on the acidification of the endosome using acridine orange staining, a pH indicator that stains acidic structures with 620 nm fluorescence (red) and nucleic acids with 520 nm fluorescence (green) (Fig. 15b) (Han and Burgess 2009; Murase et al. 2018). WT cells showed acidic endosomal organelles in red, whereas the cells treated with bafilomycin A1, a potent V-ATPase inhibitor, showed no acidic endosomes. HuR KO1 cells showed reduced red signal (620 nm fluorescence), suggesting that V-ATPase-mediated endosomal acidification was disrupted in the HuR KO cells.

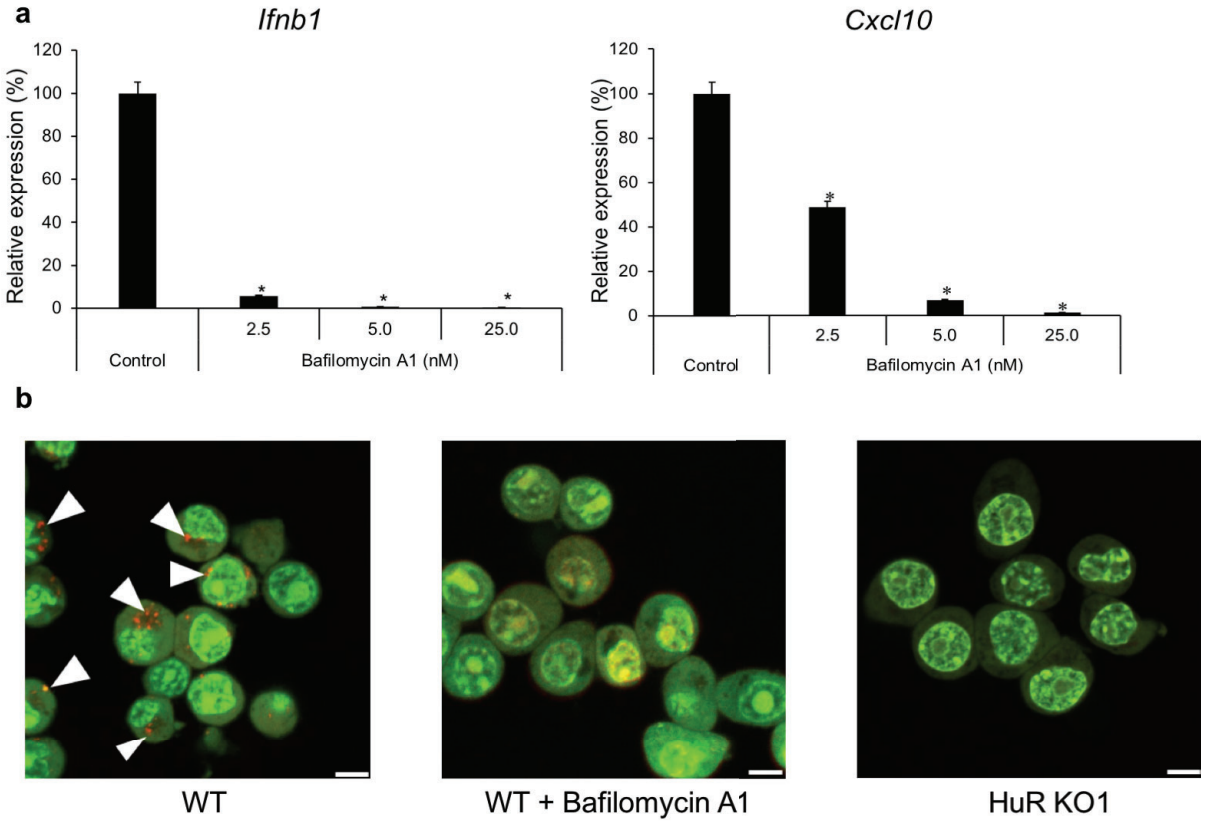


**Figure 15.** HuR regulates endosomal acidification. (**a**) RAW264.7 cells were treated with ATPase inhibitor, Bafilomycin A1 following poly(I:C) stimulation. *Ifnb1* and *Cxcl10* expression level were measured and compared to untreated cells (control). (**b**) Endosomal acidification was visualized with acridine orange staining. Red dots indicate acidified endosomes, highlighted with the white arrowheads. Left panel: WT cells; middle panel: WT cells treated with Bafilomycin A1; right panel: HuR KO1 cells. Scale bar, 10 μm. Data are the means ± SE of triplicate independent experiments. *p < 0.01, Student's t-test.

### 3.6. Atp6v0d2 KO cells show reduced TLR3 response

Our laboratory previously established Atp6v0d2 KO RAW264.7 cells and demonstrated that these cells exhibited reduced *Ifnb* and *Cxcl10* expression in response to ligands of TLR3, TLR7, and TLR9 than WT cells (Murase et al. 2018). To confirm this, I exogenously expressed FLAG-tagged Atp6v0d2 in Atp6v0d2 KO RAW264.7 cells and measured the gene expression in response to poly(I:C) stimulation in WT, Atp5v0d2 KO cells and FLAG-Atp6v0d-expressing Atp5v0d2 KO cells. Expression of FLAG–Atp6v0d2 was confirmed with WB and RT–qPCR (Fig. 16a, b). After poly(I:C) stimulation, *Ifnb1* and *Cxcl10* mRNA expressions were markedly reduced in Atp6v0d2 KO cells and were restored by FLAG–Atp6v0d2 expression (Fig. 16c), suggesting that Atp6v0d2 is required for TLR3-mediated gene expression.

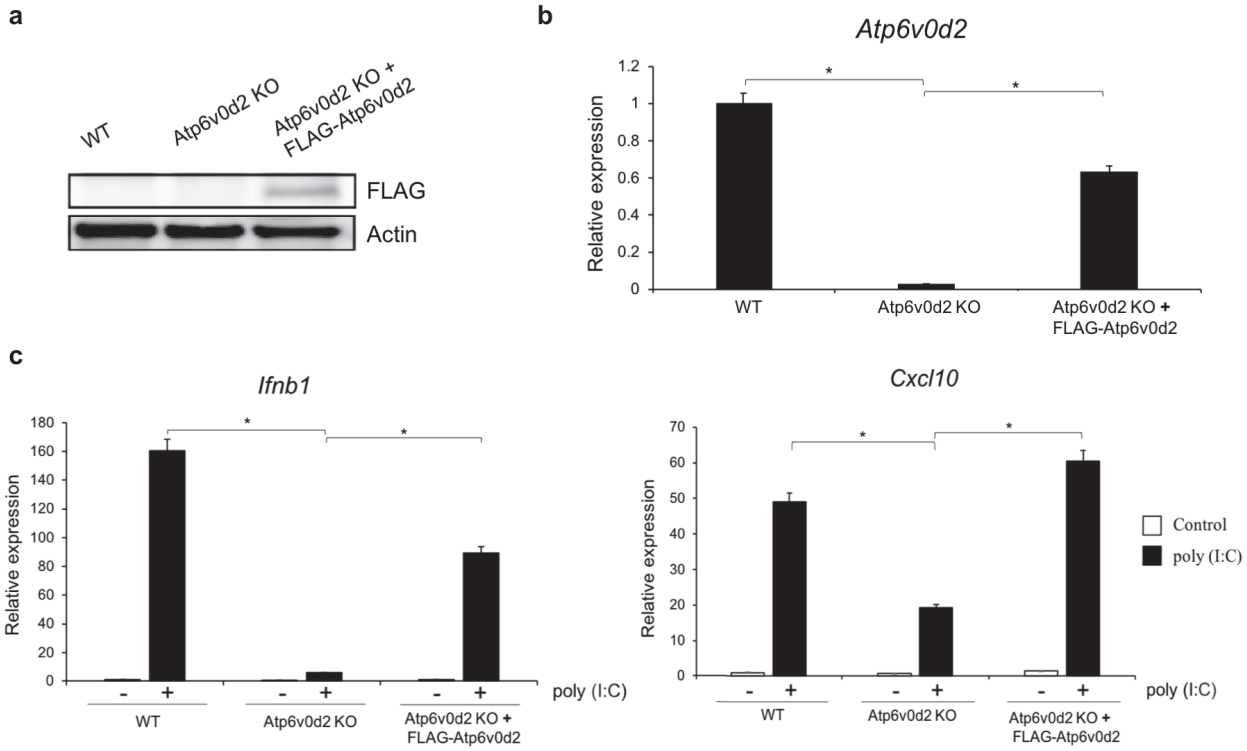


**Figure 16.** Reduced TLR3 response in *Atp6v0d2* KO cells. *Atp6v0d2* KO cells exogenously expressed FLAG–Atp6v0d2 after retroviral infection. After puromycin selection, *Atp6v0d2* expression was detected with western blotting (WB) (**a**) and RT– qPCR (**b**). (**c**) Following stimulation with poly(I:C) for 8 hours, *Ifnb1* and *Cxcl10* expression were quantified with RT–qPCR. Data are the means ± SE of triplicate independent experiments. *p < 0.01, Student's t-test.

### 3.7. HuR interacts with and stabilizes *Atp6v0d2* mRNA

To investigate whether HuR associates with *Atp6v0d2* mRNA, I performed an RNA immunoprecipitation (RIP) assay. The whole-cell lysates from RAW264.7 cells stimulated with and without poly(I:C) were immunoprecipitated with beads conjugated with control or anti-HuR antibody. *Atp6v0d2* mRNA in the precipitates was quantified with RT– qPCR. The amounts of *Atpv0d2* mRNA in the anti-HuR antibody immunoprecipitates were significantly higher than those in control antibody immunoprecipitates (Fig. 17).

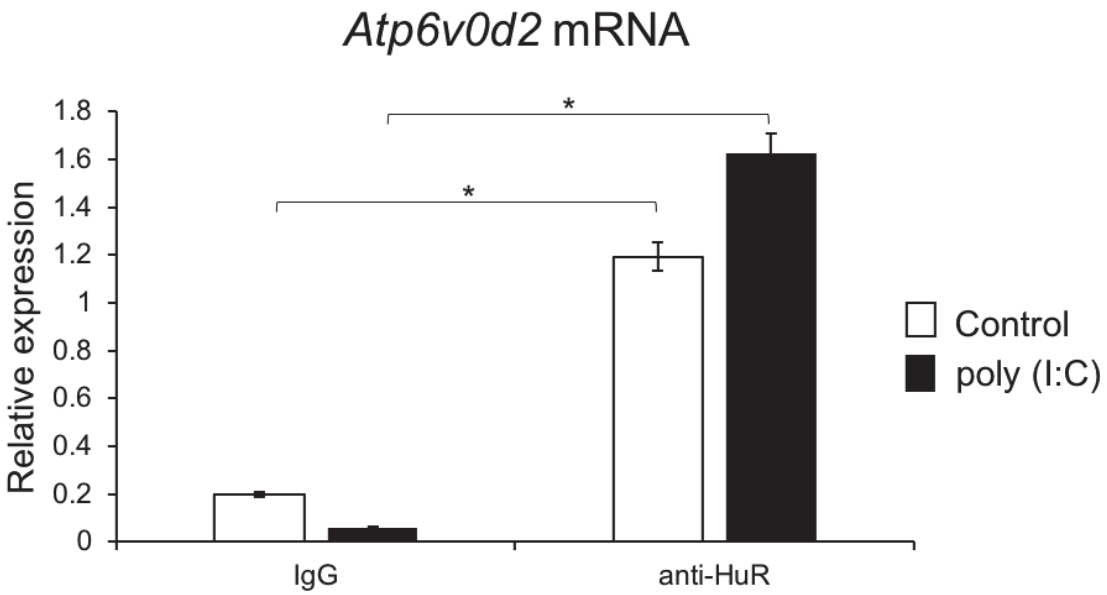


**Figure 17.** The whole-cell lysates of RAW264.7 cells treated with or without poly(I:C) stimulation for 8 hours were immunoprecipitated with control-IgG- or anti-HuR-antibody-conjugated beads. The precipitated mRNA was isolated and the bead-bound *Atp6v0d2* mRNA was quantified with RT–qPCR. Data are the means ± SE of triplicate independent experiments. *$p < 0.01$, Student's t-test.

Next, I investigated the stability of *Atp6v0d2* mRNA in the presence or absence of HuR. Poly(I:C)-stimulated WT and HuR KO RAW264.7 cells were treated with a transcriptional inhibitor, actinomycin D (2.5 μg/ml), and the time-dependent changes in mRNA after the actinomycin D treatment were quantified with RT–qPCR (Fig. 18). The half-life ($t^{1/2}$) of *Atp6v0d2* mRNA in WT cells was 118.47 min, whereas $t^{1/2}$ in HuR KO cells was 72.58 min, indicating that *Atp6v0d2* mRNA was destabilized in HuR KO cells.

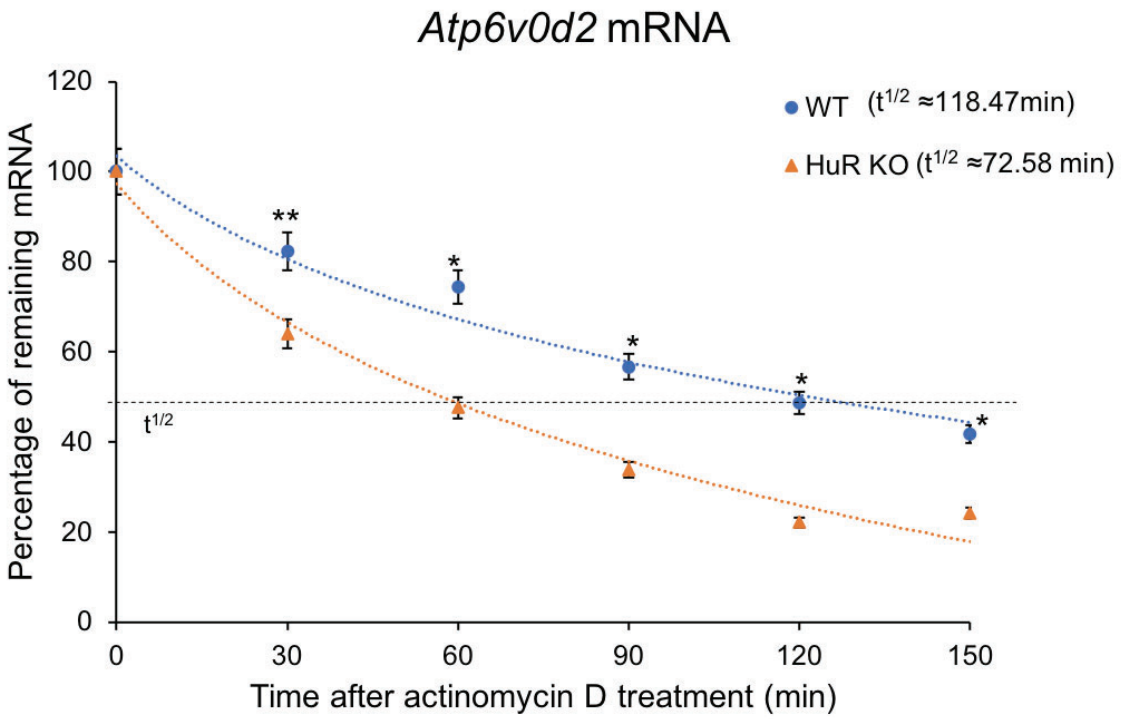


**Figure 18.** WT and HuR KO RAW264.7 cells were stimulated with poly(I:C) and treated with actinomycin D (2.5 μg/ml) for the indicated times. The amount of *Atp6v0d2* mRNA was quantified with RT–qPCR and normalized to the level of *Atp6v0d2* mRNA at time zero. Data are the means ± SE of triplicate independent experiments. *$p < 0.01$, **$p < 0.05$, Student's t-test.

I then examined whether or not the exogenous expression of HuR increases the stability of *Atp6v0d2* mRNA. HEK293T cells were transfected with or without HuR expression plasmid and treated with actinomycin D. $t^{1/2}$ of *Atp6v0d2* mRNA in HuR-overexpressing cells was 4.73 hours whereas $t^{1/2}$ in the mock-transfected cells was 2.72 hours (Fig. 19). These results suggest that HuR associates with *Atp6v0d2* mRNA and maintains its stability.

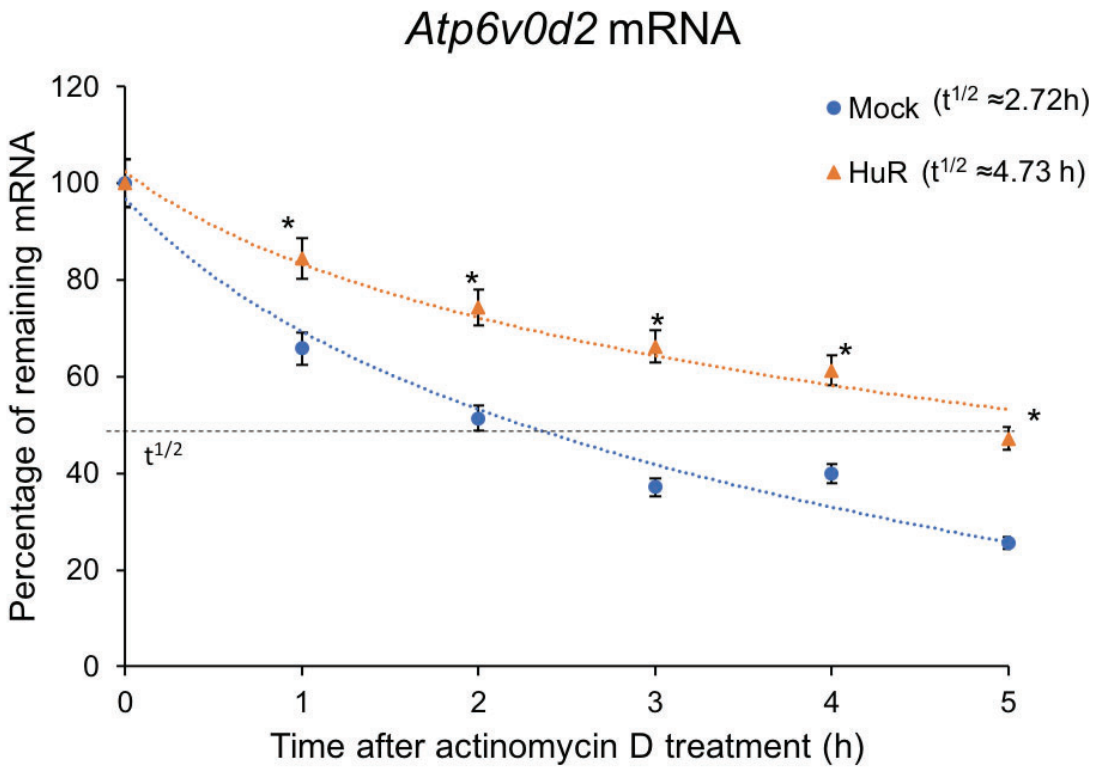


**Figure 19.** HEK293T cells were transiently transfected with empty or HuR-expressing plasmid and then stimulated for 8 hours with poly(I:C). After the medium was changed, the cells were treated with actinomycin D (5 μg/ml) for the indicated times. The amount of *Atp6v0d2* mRNA was quantified with RT– qPCR and normalized to the amount of *Atp6v0d2* mRNA at time zero. Data are the means ± SE of triplicate independent experiments. *$p < 0.01$, Student's t-test.

### 3.8. HuR binds 3'UTR of *Atp6v0d2* mRNA via the RRM domains

To examine the interaction between HuR and *Atp6v0d2* mRNA, I generated a reporter plasmid in which 3'UTR of *Atp6v0d2* mRNA (nucleotides [nt] 1123–2503 of m*Atp6v0d2* mRNA) was fused with the luciferase gene. HEK293T cells were transfected with the reporter plasmid, together with empty or FLAG-HuR-expressing plasmid. HuR overexpression significantly increased the luciferase activity in a dose-dependent manner (Fig. 20a). Because HuR contains three RRMs, I constructed deletion mutants lacking each RRM and evaluated their effects on the recognition of the 3'UTR *Atp6v0d2* mRNA by measuring the luciferase activity. Each HuR deletion mutant failed to increase the luciferase activity, suggesting that all three individual RRMs are necessary to stabilize *Atp6v0d2* mRNA (Fig. 20b).

HuR is reported to recognize AREs in mRNAs, and the 3'UTR of *Atp6v0d2* mRNA indeed contains three AREs. Therefore, I constructed a series of ARE deletion mutants in the 3'UTR of the *Atp6v0d2* mRNA expression plasmid, which lacked the sequence at nt 1867–1921 (Δmt1), nt 2101–2155 (Δmt2), or nt 2206–2270 (Δmt3). HEK293T cells were transfected individually with each of these plasmids, with or without FLAG-HuR-expressing plasmid, and the luciferase activities were measured. Luciferase activities were enhanced in the cells transfected with the full-length 3'UTR of *Atp6v0d2* (FL) reporter plasmid together with the HuR-expressing plasmid, whereas luciferase was not enhanced inΔmt1- or Δmt2-transfected cells (Fig. 20c). Δmt3-transfected cells did not show a reduction of luciferase activity. These results suggest that the RRMs in HuR associated with the sequences at nt 1867– 1921 and 2101–2155 in *Atp6v0d2* mRNA and these direct interactions are required for the HuR-mediated stabilization of *Atp6v0d2* mRNA.

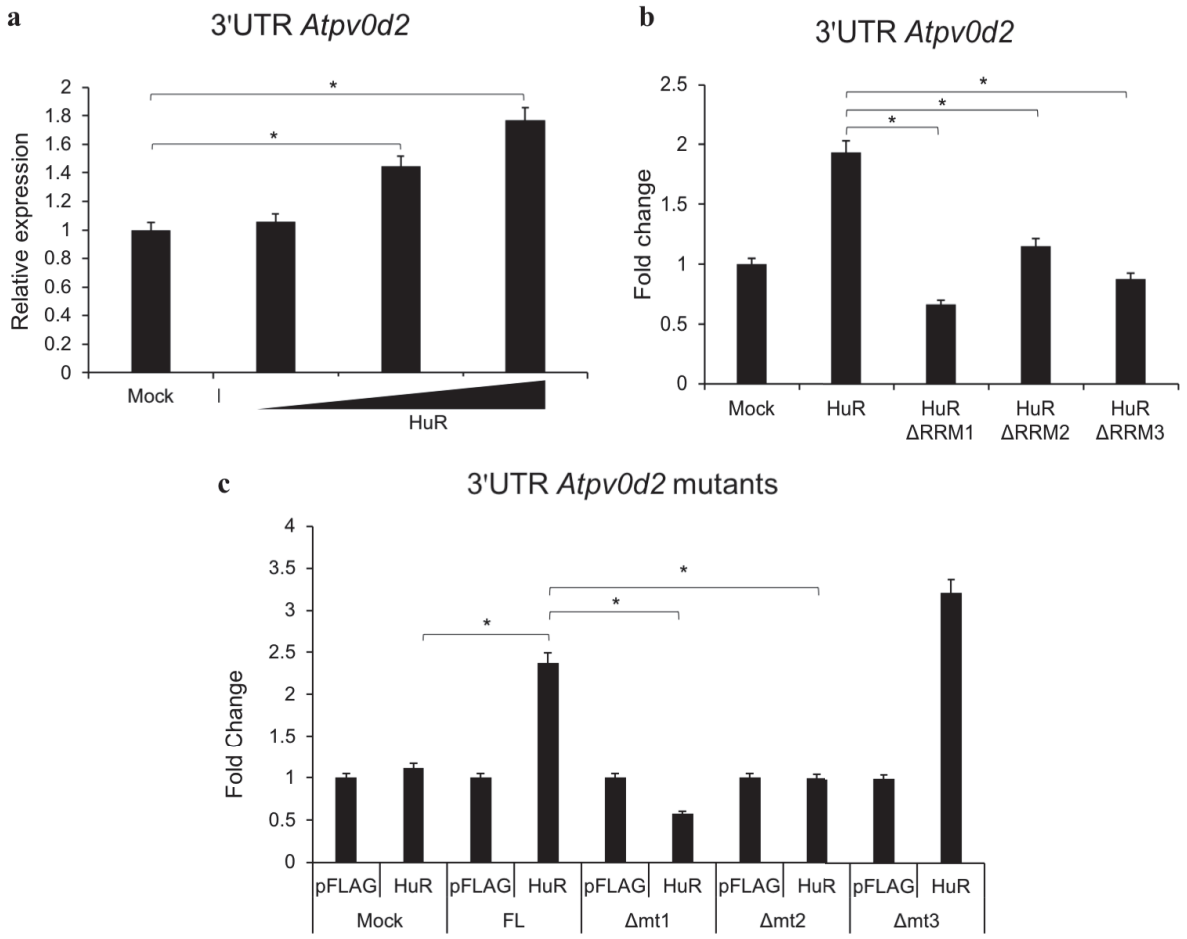


**Figure 20.** HuR interacts with 3′UTR of *Atp6v0d2* mRNA via RRMs. (**a**) HEK293T cells exogenously expressing HuR were transfected with plasmid containing the luciferase-conjugated 3′UTR of *Atp6v0d2* mRNA and the luciferase activity was measured. (**b**) HEK293T cells were transfected with plasmid containing the luciferase-conjugated 3′UTR of *Atp6v0d2* mRNA and each ΔRRM domain mutant of HuR. (**c**) HEK293T cells were transfected with plasmid containing one of the luciferase-conjugated mutants of the *Atp6v0d2* 3′UTR, with or without HuR, and the luciferase activity was measured. Data are the means ± SE of three independent experiments. *p < 0.01, Student's t-test.

## 3.9. *Atp6v0d2* expression in HuR KO cells partly restores TLR3-mediated immune response

Next, I investigated whether the reduced TLR3 responses in HuR KO cells was attributable to *Atp6v0d2* mRNA instability. I retrovirally expressed FLAG-tagged Atp6v0d2 in HuR KO RAW264.7 cells and stimulated cells with poly(I:C). The expression of FLAG–Atp6v0d2 was confirmed with WB against anti-FLAG antibody and with RT–qPCR (Fig. 21a,

b). I then stimulated WT, HuR KO, and FLAG–Atp6v0d2-expressing HuR KO cells with poly(I:C) and measured the mRNA levels of *Ifnb1* and *Cxcl10. Ifnb1* and *Cxcl10* mRNA expression were significantly reduced in the HuR KO cells compared with that in the WT cells, and these expressions were restored in the FLAG–Atp6v0d2-expressing HuR KO cells (Fig. 21c). Notably, the restoration of *Ifnb1* and *Cxcl10* mRNA expression in the FLAG–Atp6v0d2-expressing HuR KO cells was only partial compared with that in the WT cells. These results suggest that HuR at least partly regulates the TLR3-mediated innate immune responses by stabilizing the *Atp6v0d2* mRNA.

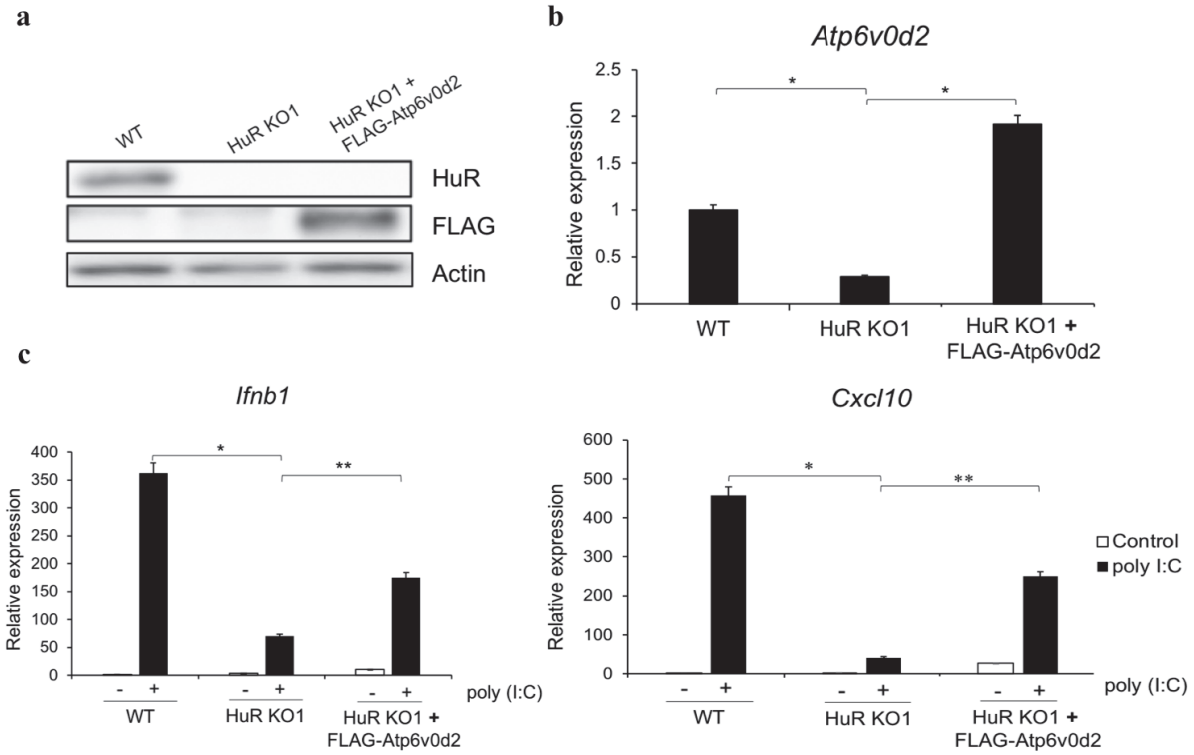


**Figure 21.** Exogenous expression of *Atp6v0d2* in HuR KO cells restored their responses to TLR3. (**a**, **b**) FLAG–Atp6v0d2 was expressed in HuR KO cells after retroviral infection and its expression was confirmed with western blotting (WB) using the indicated antibodies (**a**) and RT–qPCR (**b**). (**c**) After poly(I:C) stimulation for 8 hours, the expression levels of *Ifnb1* and *Cxcl10* mRNAs in the wild-type (WT), HuR KO1, and HuR KO1+FLAG–Atp6v0d2 cells were measured with RT–qPCR. Data are representative of three independent experiments (means ± SE). *$p < 0.01$, **$p < 0.05$, Student's t-test.

# 4. Discussion

Several lines of evidence have been suggesting that the posttranscriptional regulation of mRNA plays a pivotal role in gene expression involved in the immune responses. Shaw and Kamen demonstrated that the posttranscriptional degradation of granulocyte–macrophage colony-stimulating factor (*Csf2*) mRNA is mediated through its AU sequences (Shaw and Kamen 1986). Since then, the importance of AREs in the 3'UTR of the target mRNAs involved in innate immune regulation has been reported (Beutler et al. 1988; Caput et al. 1986; Wilson and Treisman 1988). In-depth investigations of how RBPs, such as AU-rich element RNA-binding protein 1 (AUF1), tristetraprolin (TTP), and T-cell-restricted intracellular antigen 1 (TIA1), regulate cytokine expression and the immune responses have emphasized their importance in mRNA regulation (Carballo, Lai, and Blackshear 2000; Chen et al. 2006; Lu, Sadri, and Schneider 2006; Paschoud et al. 2006; Shim et al. 2002; Wang et al. 2006; Worthington et al. 2002). HuR is one of the key players in this regulation via binding and stabilizing target mRNAs, allowing persistent protein synthesis. It has been suggested that HuR directly regulates *Il4* and *Ifnb1* mRNAs (Herdy et al. 2015; Takeuchi 2015; Yarovinsky et al. 2006).

Our laboratory previously demonstrated that HuR regulates the RLR-mediated antiviral innate immune response by increasing the stability of *Plk2* mRNA (Sueyoshi et al. 2018). PLK2 is shown to facilitate the nuclear translocation of IRF3, and therefore, HuR KO cells showed reduced IRF3 nuclear localization and subsequent antiviral responses by RNA viruses (Sueyoshi et al. 2018). Here, I extended this observation by evaluating the effects of HuR deficiency on mRNA expression after stimulation with a TLR3 agonist, and found significant reductions in *Ifnb1* and *Cxcl10* mRNA expression and in IRF3 phosphorylation in poly(I:C)-stimulated HuR KO cells. This was further supported by an HuR-shRNA-mediated knockdown analysis in which MEF and RAW264.7 cells showed reduced *Ifnb1* and *Cxcl10*

mRNA expression after poly(I:C) stimulation. Therefore, HuR regulates the antiviral innate immune response by targeting the TLR3 signaling pathway. The observations on TLR7 and TLR9 stimulation, however, showed no significant difference between WT and HuR-deficient cells. According to Yang and colleagues, poly(I:C) and LPS which are the ligands for TLR3 and TLR4 respectively, elicited a more pronounced transcriptional response than TLR9 ligand (CpG DNA), thus suggesting a preferential role of HuR in TLR3 signaling rathet than TLR9 signaling (Yang et al. 2011). Alternatively, it is possible that other RBP might be responsible for the posttranscriptional regulation of TLR7 and TLR9 signaling pathways, based on the facts that different RBPs can serve a similar function on different target molecules (Hogan et al. 2008).

Activated TLR3 is known to localize in the endosomal compartment. It is transported to the endosome from the ER via the Golgi apparatus in the presence of UNC93B1 protein (Murakami et al. 2014; Pohar et al. 2013; Qi, Singh, and Kao 2012). A number of studies have demonstrated that TLR3-mediated responses occur under acidic conditions, which are blocked by ATPase inhibitors, such as bafilomycin A1 (de Bouteiller et al. 2005; A. Kumar, Zhang, and Yu 2006; Leonard et al. 2008). In general, ligand recognition by endosomal TLRs, such as TLR3, TLR7 and TLR9, and the subsequent activation of downstream signaling are affected by the endolysosomal pH (de Bouteiller et al. 2005; Ewald et al. 2011; B. L. Lee and Barton 2014; Rutz et al. 2004). I postulated that the downregulation of the TLR3 responses by endosomal neutralization was attributable to the impairment of TLR3 cleavage, a necessary step for TLR3 and ligand ligation, or its trafficking to the endosome. Cathepsins B and Cathepsins H are two key pH-activated proteases that cleave TLR3 in endosome (Garcia-Cattaneo et al. 2012). A study by Qi et al. (2012) however, demonstrated that proteolytic cleavage is not essential for TLR3 signaling in response to poly(I:C) (Qi, Singh, and Kao 2012). Therefore, I reasoned that pH variation possibly affecting TLR3 response to ligands or

their signaling induction. In addition, TLR3 trafficking from the ER to the endosome might as well be disturbed by endosomal neutralization. Because UNC93B1 is crucial for the cytosolic trafficking of TLR3, its activity in TLR3 signaling at different pHs requires further confirmation.

Previously, we have shown that Atp6v0d2 is required for proper cytokine expression after the stimulation of the endosomal TLRs by their ligands, including TLR3, TLR7, and TLR9 (Murase et al. 2018). A deficiency of Atp6v0d2 caused the pH of the endocytic compartment of the cell to increase, thus inhibiting the activation of the endosomal TLRs. My data on RIP assay demonstrated that *Atp6v0d2* mRNA was co-precipitated with an anti-HuR antibody, suggesting that *Atp6v0d2* mRNA is a target for HuR binding. Because limited data are available on the subunits of Atp6v0d2 and its transcriptomic processing, I hypothesized that upon poly(I:C) treatment, *Atp6v0d2* mRNA becomes a critical target of HuR (among other transcripts) because it contains multiple AREs. These data establish that the ARE-containing *Atp6v0d2* mRNA is a candidate HuR target, whereas the exclusion of the other subunits warrants further investigation.

It is noteworthy that the TLR3 localization is cell type-dependent, which may reflect the critical contribution of HuR and eventually Atp6v0d2 in mediating TLR3-mediated immune response. Human fibroblast cell line is shown to express TLR3 on the cell surface instead of intracellular compartments (Vercammen, Staal, and Beyaert 2008). Therefore, the regulatory mechanism of endosomal acidification by HuR-*Atp6v0d2* mRNA interactome as modeled by the present study may not affect TLR3-mediated signaling pathway in this type of cells. Nonetheless, in most cell types, including DCs, MEFs, macrophages as well as TLR3-transfected HEK293 cells, TLR3 is predominantly localized in intracellular structure

hence dependable to HuR-*Atp6v0d2* mRNA interactome to regulate their TLR3 immune response (Matsumoto et al. 2003; Nishiya et al. 2005).

The present study suggests that HuR facilitates the TLR3-mediated innate immune response by stabilizing *Atp6v0d2* mRNA. The expression of FLAG–Atp6v0d2 in HuR KO cells resulted in the partial restoration of *Ifnb* and *Cxcl10* expression after poly(I:C) stimulation, supporting the notion that the defective responses of HuR KO cells to poly(I:C) are attributable to the increased degradation of *Atp6v0d2* mRNA. However, our previous study demonstrated that HuR KO cells showed reduced *Plk2* mRNA expression, which plays a role in potentiating IRF3 nuclear translocation during RLR signaling (Sueyoshi et al. 2018). Because IRF3 is also involved in TLR3 signaling, it is plausible that TLR3-mediated cytokine expression is only partially restored in FLAG–Atp6v0d2-expressing HuR KO because PLK2 expression is also reduced in these cells. Notably, HuR deficiency did not influence the induction of cytokine expression by TLR7 and TLR9. These TLRs do not activate IRF3, but instead activate IRF7 for induction of type I IFN. Therefore, HuR may not be essential for the activation of IRF7 during TLR7 and TLR9 signaling. However, unlike HuR KO cells, which show the normal induction of *Ifnb* and *Cxcl10* mRNAs by TLR7 and TLR9 ligands, Atp6v0d2 KO cells show defective expression of these genes (Murase et al. 2018). Therefore, it is possible that although *Atp6v0d2* expression is reduced in HuR KO cells, the acidification of the intracellular vesicles is only partially affected and insufficient to impede the robust functions of TLR7 and TLR9, such as their trafficking to endosome or proteolytic cleavage. Thus, HuR may regulate TLR3-mediated antiviral innate immunity by targeting both *Atp6v0d2* and *Plk2* mRNAs.

The posttranscriptional regulation of the TLR-mediated immune response is essential to the generation of a proper signaling cascade after stimulation by specific ligands. In the

host, particular caution is required in activating nucleic-acid-sensing TLRs, such as TLR3, TLR7 and TLR9, to avoid self-recognition and thus the induction of autoimmunity. This may be one of the reasons why all nucleic-acid sensors localize to an endocytic compartment, such as the endolysosome, to allow their activities to be monitored. A critical aspect of the regulation of nucleic-acid-recognizing TLRs is their trafficking and targeting to endosomes (Chaturvedi and Pierce 2009; Lee and Barton 2014). HuR, as a posttranscriptional regulator of mRNAs, seems to play some roles in this regulatory mechanism. My data suggest that HuR contributes to the endocytic regulatory machinery by targeting the ATPase subunit involved in the acidification process, which in turn governs the responsiveness of nucleic-acid-sensing TLRs, particularly TLR3. This alternative route of TLR3 activity demonstrates the complex regulatory mechanisms of TLR3, which can be manipulated to formulate new antiviral drugs for optimal effects.

Overall, the present study demonstrated that HuR recognizes *Atp6v0d2* mRNA via ARE site in 3'UTR and stabilizes it upon poly(I:C) stimulation. The stabilization promotes endosomal acidification, which is crucial in triggering TLR3 signaling pathway. On the other hand, HuR deficiency suppressed *Atp6v0d2* mRNA expression by promoting immediate mRNA degradation, which subsequently disrupts endosomal acidification. As a result, without appropriate acidic condition, endosomal activities were affected, hence reduced TLR3-mediated signaling pathway. In conclusion, HuR plays a pivotal role in TLR3-mediated immune response by targeting V-ATPase functionality to regulates endosomal acidification.

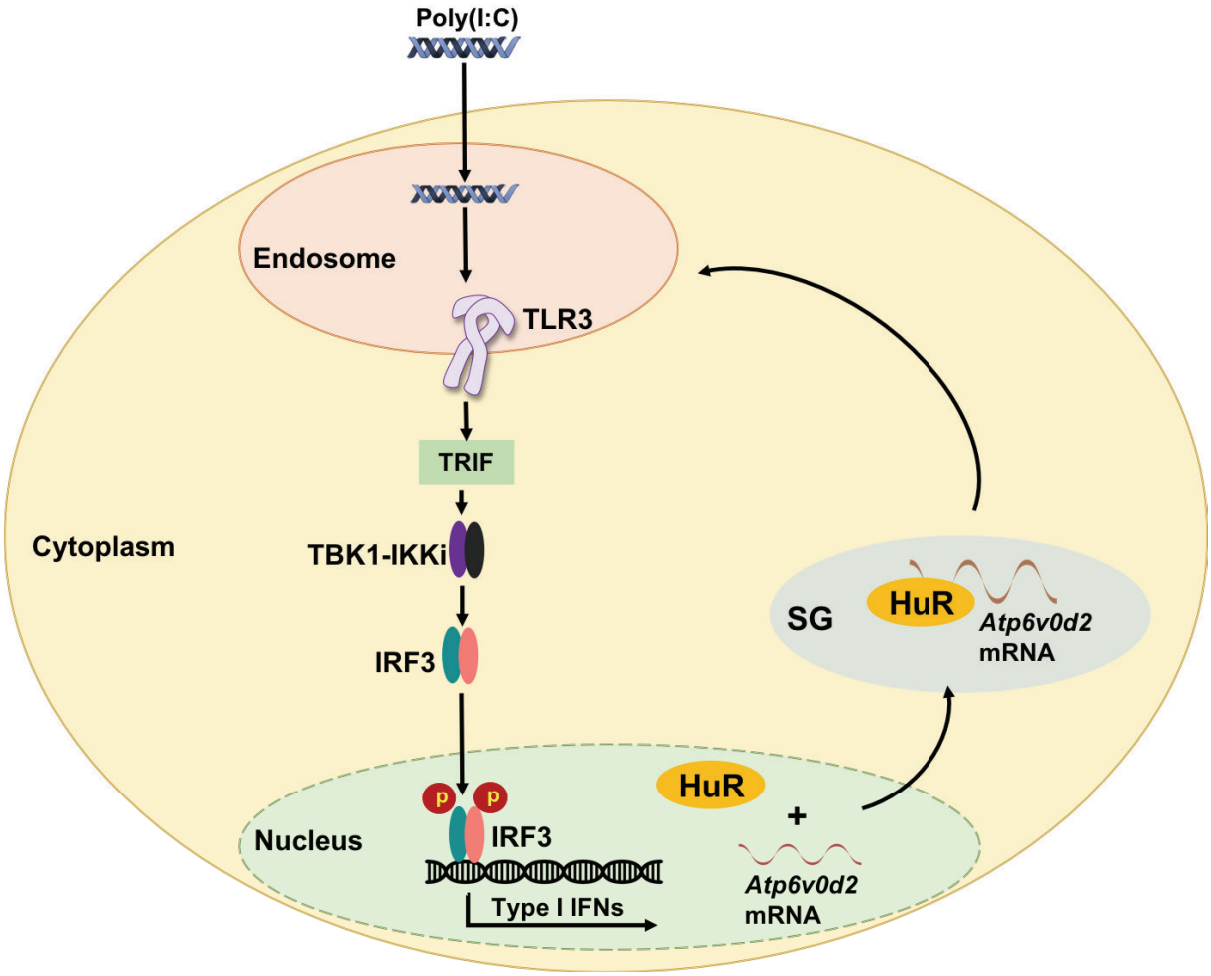


**Figure 22.** Following poly(I:C) stimulation, HuR binds *Atp6v0d2* mRNA in the nucleus and translocates into cytoplasmic stress granule (SG) to facilitate mRNA stabilization. The assembly of HuR-mRNA interactome subsequently promotes endosomal acidification, a condition required for TLR3 activation to induce type 1 interferons production.

# 5. Acknowledgements

I am very grateful to first and foremost thank my Ph.D. supervisor Professor Taro Kawai. He provided me the valuable opportunity to conduct my Ph.D. research in his laboratory. Throughout four fruitful years, his endless guidance, scientific discussion, and critics inspired me to accomplish my Ph.D. objectives and research goals, especially in mastering molecular biology techniques and understanding innate immunity. Special thanks to the Assistant Professor Takumi Kawasaki for the supervision, dedication, and encouragement throughout my study. He was a great mentor and teacher who always guided me through my laboratory experiments, solving technical problems, and data analyses.

Also, thank you to all members in Molecular Immunobiology lab for the invaluable help, supports, and ideas. I am very thankful for the aids from Japanese students and staffs who assisted me in my daily life as a foreigner in The Land of The Rising Sun, especially in overcoming the language barrier. The language translation and cultural explanations were very much appreciated. For the technical staffs at Biological Science Divisions and secretaries, Mdm. Chihiro Suzuki and Mdm. Kayo Abe, thank you for all the assistance. Many thanks also extended to former lab members Dr. Dyaningtyas Dewi Pamungkas Putri, Dr. Motoya Murase, Dr. Takuya Sueyoshi and Dr. Hasan Md Zobaer for scientific advice and reference.

I would like to thank my thesis advisors, Professor Naoyuki Inagaki and Associate Professor Yasumasa Ishida for their scientific insights and encouragements. Their valuable comments and critics had guided me to improve my research performance. A token of gratitude also extended to MEXT for their financial support through Monbukagakusho scholarship. Last but not least, my family deserve thanks beyond expression for their love, emotional encouragement, financial assistance, and supports in any way possible.

**Mohd Izwan Bin Zainol**
Nara, July 2019

# 6. Reference


Barral, Paola M et al. 2009. “Functions of the Cytoplasmic RNA Sensors RIG-I and MDA-5: Key Regulators of Innate Immunity.” *Pharmacology & therapeutics* 124(2): 219–34. https://www.ncbi.nlm.nih.gov/pubmed/19615405.

Beutler, Bruce et al. 1988. “Assay of a Ribonuclease That Preferentially Hydrolyses MRNAs Containing Cytokine-Derived UA-Rich Instability Sequences.” *Biochemical and biophysical research communications* 152(3): 973–80.

Blasius, Amanda L, and Bruce Beutler. 2010. “Intracellular Toll-like Receptors.” *Immunity* 32(3): 305–15.

Bley, Nadine et al. 2015. “Stress Granules Are Dispensable for MRNA Stabilization during Cellular Stress.” *Nucleic acids research* 43(4): e26–e26. https://www.ncbi.nlm.nih.gov/pubmed/25488811.

de Bouteiller, Odette et al. 2005. “Recognition of Double-Stranded RNA by Human Toll-like Receptor 3 and Downstream Receptor Signaling Requires Multimerization and an Acidic PH.” *Journal of Biological Chemistry* 280(46): 38133–45.

Brennan, C M, and J A Steitz. 2001. “HuR and MRNA Stability.” *Cellular and molecular life sciences CMLS* 58(2): 266–77.

Brinkmann, Melanie M et al. 2007. “The Interaction between the ER Membrane Protein UNC93B and TLR3, 7, and 9 Is Crucial for TLR Signaling.” *The Journal of cell biology* 177(2): 265–75.

Caput, D et al. 1986. “Identification of a Common Nucleotide Sequence in the 3’-Untranslated Region of MRNA Molecules Specifying Inflammatory Mediators.” *Proceedings of the National Academy of Sciences* 83(6): 1670–74.

Carballo, E, W S Lai, and P J Blackshear. 2000. “Evidence That Tristetraprolin Is a Physiological Regulator of Granulocyte-Macrophage Colony-Stimulating Factor

Messenger RNA Deadenylation and Stability." *Blood* 95(6): 1891–99.

Chaturvedi, Akanksha, and Susan K Pierce. 2009. "How Location Governs Toll-like Receptor Signaling." *Traffic* 10(6): 621–28.

Chen, Yu-Ling et al. 2006. "Differential Regulation of ARE-Mediated TNFalpha and IL-1beta MRNA Stability by Lipopolysaccharide in RAW264.7 Cells." *Biochemical and biophysical research communications* 346(1): 160–68.

Cotter, Kristina, Laura Stransky, Christina McGuire, and Michael Forgac. 2015. "Recent Insights into the Structure, Regulation, and Function of the V-ATPases." *Trends in biochemical sciences* 40(10): 611–22.

Cross, Richard L, and Volker Muller. 2004. "The Evolution of A-, F-, and V-Type ATP Synthases and ATPases: Reversals in Function and Changes in the H+/ATP Coupling Ratio." *FEBS letters* 576(1–2): 1–4.

Dauletbaev, Nurlan, Maria Cammisano, Kassey Herscovitch, and Larry C Lands. 2015. "Stimulation of the RIG-I/MAVS Pathway by Polyinosinic:Polycytidylic Acid Upregulates IFN-β in Airway Epithelial Cells with Minimal Costimulation of IL-8." *The Journal of Immunology* 195(6): 2829 LP – 2841. http://www.jimmunol.org/content/195/6/2829.abstract.

Diebold, Sandra Stephanie, and Eva Brencicova. 2013. "Nucleic Acids and Endosomal Pattern Recognition: How to Tell Friend from Foe?" *Frontiers in cellular and infection microbiology* 3: 37.

Ewald, Sarah E et al. 2011. "Nucleic Acid Recognition by Toll-like Receptors Is Coupled to Stepwise Processing by Cathepsins and Asparagine Endopeptidase." *The Journal of experimental medicine* 208(4): 643–51.

Fan, Xinhao Cynthia, and Joan A Steitz. 1998. "HNS, a Nuclear-Cytoplasmic Shuttling Sequence in HuR." *Proceedings of the National Academy of Sciences* 95(26): 15293–98.

Forgac, Michael. 2007. “Vacuolar ATPases: Rotary Proton Pumps in Physiology and Pathophysiology.” *Nature reviews. Molecular cell biology* 8(11): 917–29.

Garcia-Cattaneo, Alejandra et al. 2012. “Cleavage of Toll-like Receptor 3 by Cathepsins B and H Is Essential for Signaling.” *Proceedings of the National Academy of Sciences* 109(23): 9053–58.

Gleeson, Paul A. 2014. “The Role of Endosomes in Innate and Adaptive Immunity.” In *Seminars in Cell & Developmental Biology*, Elsevier, 64–72.

Han, Junyan, and Kevin Burgess. 2009. “Fluorescent Indicators for Intracellular PH.” *Chemical reviews* 110(5): 2709–28.

Herdy, Barbara et al. 2015. “The RNA-Binding Protein HuR/ELAVL1 Regulates IFN-Beta MRNA Abundance and the Type I IFN Response.” *European journal of immunology* 45(5): 1500–1511.

Hinman, M N, and H Lou. 2008. “Diverse Molecular Functions of Hu Proteins.” *Cellular and molecular life sciences* 65(20): 3168.

Hogan, Daniel J et al. 2008. “Diverse RNA-Binding Proteins Interact with Functionally Related Sets of RNAs, Suggesting an Extensive Regulatory System” ed. Sean R. Eddy. *PLoS Biology* 6(10): e255. https://dx.plos.org/10.1371/journal.pbio.0060255 (June 24, 2019).

Huss, Markus, and Helmut Wieczorek. 2009. “Inhibitors of V-ATPases: Old and New Players.” *The Journal of experimental biology* 212(Pt 3): 341–46.

Jensen, Søren, and Allan Randrup Thomsen. 2012. “Sensing of RNA Viruses: A Review of Innate Immune Receptors Involved in Recognizing RNA Virus Invasion.” *Journal of Virology* 86(6): 2900 LP – 2910. http://jvi.asm.org/content/86/6/2900.abstract.

Katsanou, Vicky et al. 2009. “The RNA-Binding Protein Elavl1/HuR Is Essential for Placental Branching Morphogenesis and Embryonic Development.” *Molecular and*

*cellular biology* 29(10): 2762–76.

Kawai, Taro, and Shizuo Akira. 2010. "The Role of Pattern-Recognition Receptors in Innate Immunity: Update on Toll-like Receptors." *Nature immunology* 11(5): 373. https://www.nature.com/articles/ni.1863.

Kim, You-Me, Melanie M Brinkmann, Marie-Eve Paquet, and Hidde L Ploegh. 2008. "UNC93B1 Delivers Nucleotide-Sensing Toll-like Receptors to Endolysosomes." *Nature* 452(7184): 234–38.

Kitai, Yuichi et al. 2015. "Negative Regulation of Melanoma Differentiation-Associated Gene 5 (MDA5)-Dependent Antiviral Innate Immune Responses by Arf-like Protein 5B." *Journal of Biological Chemistry* 290(2): 1269–80.

Kumar, Ashok, Jing Zhang, and Fu-Shin X Yu. 2006. "Toll-like Receptor 3 Agonist Poly (I: C)-induced Antiviral Response in Human Corneal Epithelial Cells." *Immunology* 117(1): 11–21.

Kumar, Himanshu, Taro Kawai, and Shizuo Akira. 2009. "Toll-like Receptors and Innate Immunity." *Biochemical and biophysical research communications* 388(4): 621–25.

Lal, Ashish et al. 2004. "Concurrent versus Individual Binding of HuR and AUF1 to Common Labile Target MRNAs." *The EMBO journal* 23(15): 3092–3102.

Lee, Bettina L, and Gregory M Barton. 2014. "Trafficking of Endosomal Toll-like Receptors." *Trends in cell biology* 24(6): 360–69.

Lee, Clarissa C, Ana M Avalos, and Hidde L Ploegh. 2012. "Accessory Molecules for Toll-like Receptors and Their Function." *Nature reviews. Immunology* 12(3): 168–79.

Leonard, Joshua N et al. 2008. "The TLR3 Signaling Complex Forms by Cooperative Receptor Dimerization." *Proceedings of the National Academy of Sciences* 105(1): 258–63.

Lu, Jin-Yu, Navid Sadri, and Robert J Schneider. 2006. "Endotoxic Shock in AUF1

Knockout Mice Mediated by Failure to Degrade Proinflammatory Cytokine MRNAs." *Genes & development* 20(22): 3174–84.

Marshansky, Vladimir, and Masamitsu Futai. 2008. "The V-Type H+-ATPase in Vesicular Trafficking: Targeting, Regulation and Function." *Current opinion in cell biology* 20(4): 415–26.

Matsumoto, Misako et al. 2003. "Subcellular Localization of Toll-like Receptor 3 in Human Dendritic Cells." *Journal of immunology (Baltimore, Md. : 1950)* 171(6): 3154–62.

Maxson, Michelle E, and Sergio Grinstein. 2014. "The Vacuolar-Type $H^+$-ATPase at a Glance - More than a Proton Pump." *Journal of Cell Science* 127(23): 4987 LP – 4993. http://jcs.biologists.org/content/127/23/4987.abstract.

Mellman, I, and G Warren. 2000. "The Road Taken: Past and Future Foundations of Membrane Traffic." *Cell* 100(1): 99–112.

Meylan, Etienne, and Jürg Tschopp. 2006. "Toll-Like Receptors and RNA Helicases: Two Parallel Ways to Trigger Antiviral Responses." *Molecular Cell* 22(5): 561–69. http://www.sciencedirect.com/science/article/pii/S1097276506003273.

Mukherjee, Neelanjan et al. 2011. "Integrative Regulatory Mapping Indicates That the RNA-Binding Protein HuR Couples Pre-MRNA Processing and MRNA Stability." *Molecular cell* 43(3): 327–39.

Murakami, Yusuke et al. 2014. "Roles of the Cleaved N-Terminal TLR3 Fragment and Cell Surface TLR3 in Double-Stranded RNA Sensing." *The Journal of Immunology* 193(10): 5208 LP – 5217. http://www.jimmunol.org/content/193/10/5208.abstract.

Murase, Motoya et al. 2018. "Intravesicular Acidification Regulates Lipopolysaccharide Inflammation and Tolerance through TLR4 Trafficking." *The Journal of Immunology* 200(8): 2798–2808.

Nishiya, Tadashi, Emi Kajita, Soichi Miwa, and Anthony L DeFranco. 2005. "TLR3 and

TLR7 Are Targeted to the Same Intracellular Compartments by Distinct Regulatory Elements." *Journal of Biological Chemistry* 280(44): 37107–17. http://www.jbc.org/content/280/44/37107.abstract.

Paschoud, Serge et al. 2006. "Destabilization of Interleukin-6 MRNA Requires a Putative RNA Stem-Loop Structure, an AU-Rich Element, and the RNA-Binding Protein AUF1." *Molecular and cellular biology* 26(22): 8228–41.

Pohar, Jelka et al. 2013. "The Role of UNC93B1 Protein in Surface Localization of TLR3 Receptor and in Cell Priming to Nucleic Acid Agonists." *Journal of Biological Chemistry* 288(1): 442–54.

Protter, David S W, and Roy Parker. 2016. "Principles and Properties of Stress Granules." *Trends in cell biology* 26(9): 668–79. https://www.ncbi.nlm.nih.gov/pubmed/27289443.

Qi, Rongsu, Divyendu Singh, and C Cheng Kao. 2012. "Proteolytic Processing Regulates Toll-like Receptor 3 Stability and Endosomal Localization." *Journal of Biological Chemistry* 287(39): 32617–29.

Rutz, Mark et al. 2004. "Toll-like Receptor 9 Binds Single-stranded CpG-DNA in a Sequence-and PH-dependent Manner." *European journal of immunology* 34(9): 2541–50.

Scheiba, Rafael M et al. 2014. "The C-Terminal RNA Binding Motif of HuR Is a Multi-Functional Domain Leading to HuR Oligomerization and Binding to U-Rich RNA Targets." *RNA biology* 11(10): 1250–61.

Shaw, Gray, and Robert Kamen. 1986. "A Conserved AU Sequence from the 3′ Untranslated Region of GM-CSF MRNA Mediates Selective MRNA Degradation." *Cell* 46(5): 659–67.

Shim, Jaekyung, Hanjo Lim, John R Yates, and Michael Karin. 2002. "Nuclear Export of NF90 Is Required for Interleukin-2 MRNA Stabilization." *Molecular cell* 10(6): 1331–

44.

Sueyoshi, Takuya et al. 2018. “Hu Antigen R Regulates Antiviral Innate Immune Responses through the Stabilization of MRNA for Polo-like Kinase 2.” *The Journal of Immunology* 200(11): 3814–24.

Sun-Wada, Ge-Hong, Yoh Wada, and Masamitsu Futai. 2004. “Diverse and Essential Roles of Mammalian Vacuolar-Type Proton Pump ATPase: Toward the Physiological Understanding of inside Acidic Compartments.” *Biochimica et Biophysica Acta (BBA)-Bioenergetics* 1658(1–2): 106–14.

Takeuchi, Osamu. 2015. “HuR Keeps Interferon-Beta MRNA Stable.” *European journal of immunology* 45(5): 1296–99.

Vercammen, Elisabeth, Jens Staal, and Rudi Beyaert. 2008. “Sensing of Viral Infection and Activation of Innate Immunity by Toll-like Receptor 3.” *Clinical microbiology reviews* 21(1): 13–25.

Wang, Jin Gene et al. 2006. “LFA-1-Dependent HuR Nuclear Export and Cytokine MRNA Stabilization in T Cell Activation.” *Journal of immunology (Baltimore, Md. : 1950)* 176(4): 2105–13.

Wilson, Tim, and Richard Treisman. 1988. “Removal of Poly (A) and Consequent Degradation of c-Fos MRNA Facilitated by 3′ AU-Rich Sequences.” *Nature* 336(6197): 396.

Worthington, Mark T et al. 2002. “RNA Binding Properties of the AU-Rich Element-Binding Recombinant Nup475/TIS11/Tristetraprolin Protein.” *The Journal of biological chemistry* 277(50): 48558–64.

Yang, Ivana V et al. 2011. “Identification of Novel Innate Immune Genes by Transcriptional Profiling of Macrophages Stimulated with TLR Ligands.” *Molecular immunology* 48(15–16): 1886–95.

Yarovinsky, Timur O, Noah S Butler, Martha M Monick, and Gary W Hunninghake. 2006. "Early Exposure to IL-4 Stabilizes IL-4 MRNA in CD4+ T Cells via RNA-Binding Protein HuR." *Journal of immunology (Baltimore, Md. : 1950)* 177(7): 4426–35.